STUDY OF NON-LINEAR RESPONSE OF SOME PARAMETRIC OSCILLATORS WITH VIBRATIONAL RESONANCE

A thesis presented for the degree of

Doctor of Philosophy

SOMNATH ROY

201/18/Phys/26

Department of Physics

Jadavpur University

West Bengal, Kolkata-700032

JADVPUR UNIVERSITY

DEPARTMENT OF PHYSICS

CERTIFICATE FROM THE SUPERVISOR

THIS IS TO CERTIFY THAT THE THESIS ENTITLED "**STUDY OF NON-LINEAR RESPONSE OF SOME PARAMETRIC OSCILLATORS WITH VIBRATIONAL RESONANCE** " SUBMITTED BY "**SRI SOMANTH ROY**" WHO GOT HIS NAME REGISTERED ON **24TH SEPTEMBER 2018** FOR THE AWARD OF **PH.D. (SIENCE)** DEGREE OF **JADAVPUR UNIVERSITY**, IS ABSOLUTELY BASED UPON HIS OWN WORK UNDER THE SUPERVISION OF **DR.DHRUBA BANERJEE** AND NEITHER THIS THESIS NOR ANY PART OF IT HAS BEEN SUBMITTED FOR ANY DEGREE/DIPLOMA OR ANY OTHER ACADEMIC AWARD ANYWHERE BEFORE.

Dhruba Banerjee

19-05-2022

Supervisor

Dr. Dhruba Banerjee

Dr. DHRUBA BANERJEE
Assistant Professor
Dept. of Physics
JADAVPUR UNIVERSITY
KOLKATA - 700 032

ABSTRACT

INDEX NO-201/18/Phys/26

Title: Study of Non-Linear Response of Some Parametric Oscillators With Vibrational Resonance.

This Ph.D. thesis consists of the analysis of nonlinear response of certain oscillators under the influence of bi-harmonic forces of widely different frequencies (slow and fast frequency). In literature, study of resonance response by controlling this fast frequency drive strength is extensively known as ***Vibrational Resonance***.

We consider various types of parametric oscillators for this purpose. In our study of Mathieu-Duffing oscillator and Van der Pol-Mathieu-Duffing oscillator, we examine the effects of fast frequency and fast drive strength on the system's response to the external slow excitation. We also inspect the behavior of system's stability through bifurcation analysis by tuning the fast drive frequency. To derive the analytical results we use perturbation methods like direct partition of motion, multiple time scale analysis, Lindstedt-Poincaré method of perturbation. Finally, all the analytical results are supported by the detailed numerical simulations and physical interpretations are given.

Signature of the candidate

Somnath Roy
19/05/2022

Somnath Roy

Signature of the supervisor

Dhruba Banerjee 19-05-2022

Dr. DHRUBA BANERJEE
Assistant Professor
Dept. of Physics
JADAVPUR UNIVERSITY
KOLKATA - 700 032

Dr. Dhruba Banerjee

Assistant Professor.

Jadavpur University.

Kolkata- 700032.

Author's Delaration

I declare that the work in this dissertation was carried out in accordance with the requirements of the University's regulations and code of practice for research degree programmes and that it has not been submitted for any other academic award. Except where indicated by specific reference in the text, the work is my own work. Work done in collaboration with, or with the assistance of others is indicated as such. Any views expressed in the dissertation are those of the authors.

Somnath Roy

19/05/2022

Somnath Roy.

Dedications

TO
ALL OF MY TEACHERS.

Acknowledgement

A Doctor of Philosophy known as Ph.D. comes from the Latin "**To Teach**" and Greek "**Love of Wisdom**." It is a process where one means to master ins and outs of a topic that is really of one's interest. A process to learn and expand knowledge and really get to know what something is about. These five years of my journey will not have come to this stunning conclusion without the constant support of my supervisor **Dr. Dhruba Banerjee**. My gratitude to him is beyond words. Honestly speaking, he is more than just a 'Supervisor'; instead, he is remembered as one of the most exemplary teachers for the rest of my life. Pursuing "Nonlinear Dynamics" as my research stream also impacted his teaching of the particular course in my post-graduate curriculum. Not only this topic, but his immense capability to connect physical results to detailed mathematical interpretation is also an eye-opener to everyone who participated in his class. Moreover, his deep understanding and intuition of a specific problem was my savior many times in these years, and I hope it will be in the future.

I would like to mention here **Dr. Arabinda Chowdhury**(Seth Anandram Jaipuria College, Kolkata), my undergraduate teacher in my college; without his support, my part of the journey wouldn't be meaningful. I still remember his delightful teaching and extraordinary insight into laboratory experiments in my college days. Even in my research, whenever I stuck with some numerical analysis, his knowledge in programming, especially in Python, helped

me a lot so often that I couldn't describe it in words.

I would like to acknowledge **Dr. Tanmoy Paul** (Chandernagore Government College) for being a part of this beautiful journey; from a roommate to a splendid friend and an inspiring guide whose constant encouragement and suggestions helps me a lot during these years.

I feel blessed to have the companions, my seniors, and my co-author Chitrak Da, Jyotipriya Da, and Debapriya Di. It never felt like an "out of zone environment" to me in their presence. I recall those days with Chitrak Da when we walked for hours around the university campus in the evening and discussed so many things that remain wonderful memories throughout my life.

Truly said *"There are friends, there is family, and then there are friends that become family"*. A part of my journey is dedicated to them. *Rohit, Debjit, Subhamita, Ankita, Anupa, Ratna* we were the wolfpacks during our university days. Our days seemed incomplete without the evening 'adda' at 'Suruchi' canteen. After every semester, our 'exploring Kolkata tour' was a mandatory one.
Finally, it will not be justice to this paragraph if I do not mention the names *Santanu, Bhaskar, Tanmoy Da*. They become more than a friend to me. Every word is less to describe how they influence my life during this course. I can just say *THANK YOU*, guys, for being here, for giving meaning to my life.

All these words written here are not possible without my family: Ma, Baba, Didi, and my wife, Gargi. Without their constant emotional support in every step of my life and encouragement for every decision I took, the part of this academic voyage might not have reached a meaningful conclusion.

List Of Publications

1. **Nonlinear response of a parametric bistable oscillator with multiple excitations.**
   Somnath Roy, Debapriya Das, Dhruba Banerjee
   Nonlinear response of a parametric bistable oscillator with multiple excitations. Eur. Phys. J. B 93, 12 (2020).

2. **Vibrational resonance in a bistable van der Pol–Mathieu–Duffing oscillator.**
   Somnath Roy, Debapriya Das, Dhruba Banerjee
   International Journal of Non-Linear Mechanics, Volume 135, October 2021, 103771

3. **Vibrational response of a parametric bistable oscillator.**
   Somnath Roy, Dhruba Banerjee
   Presented in ***3rd National seminar on nonlinear and complex phenomenon (NCP-2020)***,
   Jadavpur University.

4. **Supercritical Hopf Bifurcation in vibrational resonance through modulation of fast frequency.** (Communicated)
   Somnath Roy, Debapriya Das, Dhruba Banerjee

Contents

List of Figures

Chapter 1

Vibration and resonance in engineering and natural science

1.1 Resonance in linear and non-linear systems

Resonance is one of the elemental marvels shown by nonlinear systems and is imperative in material science, engineering, and almost all other fields of natural sciences. It alludes to a realization of the maximum response of a dynamical framework. In a vibrating framework, the response is basically due to the capacity of the system to store and exchange energy received from an outside driving source into an inside vibrational mode. Resonance can be deterministic or stochastic(random) and can be realized in microscopic and

macroscopic systems. Both single and coupled dynamical systems can show resonance behavior. It is beneficial in numerous applications and additionally leads to instability and catastrophes in certain systems.For certain sorts of nonlinear frameworks, especially oscillators with polynomial type potentials or forces, it is conceivable to get an inexact hypothetical expression for the swaying amplitude and after that one can dissect the event of resonance as well impact of different parameters on the resonance.Analysis of resonance is non trivial when the systems are inherently nonlinear and needs knowledge of various perturbation scheme.In the next subsection we are going to review a extensively used perturbation technique namely *multiple time scale analysis*.

1.1.1 Multiple Time Scale Analysis: A brief review

Before going to elaborate discussions on the resonance of a typical nonlinear oscillator, let us review a particular perturbation scheme, *multiple time scale analysis*, which we have used frequently in our study to solve various nonlinear integro-differential equations.

Comparison with asymptotic expansion

Let us pick an example of a damped harmonic oscillator as its exact solution is known and easy to compare with the approximate solution.

$$\ddot{x} + x = -2\epsilon\dot{x} \tag{1.1.1.1}$$

By considering the asymptotic expansion with small perturbative parameter $\epsilon < 1$

$$x = x_0 + \epsilon x_1 + \epsilon^2 x_2 + ... \tag{1.1.1.2}$$

Substituting Eq.(1.1.1.2) into Eq.(1.1.1.1) and equating the coefficients of ϵ to the same power,

$$\mathcal{O}(\epsilon^0): \qquad \ddot{x_0} + x_0 = 0 \tag{1.1.1.3}$$

$$\mathcal{O}(\epsilon^1): \quad \ddot{x_1} + x_1 = -2\dot{x_0} \tag{1.1.1.4}$$

$$\mathcal{O}(\epsilon^2): \quad \ddot{x_2} + x_2 = -2\dot{x_1} \tag{1.1.1.5}$$

Zeroth order gives the harmonic solution as;

$$x_0 = a\cos(t + \theta) \tag{1.1.1.6}$$

where a and θ are amplitude and phase respectively.Now putting Eq.(1.1.1.6) into Eq.(1.1.1.5) we can get the solution for x_1,

$$x_1 = -at\cos(t + \theta). \tag{1.1.1.7}$$

Finally substituting Eq.(1.1.1.7) into Eq.(1.1.1.6) we arrive at the solution for x_2

$$x_2 = \frac{1}{2}at^2\cos(t+\theta) + \frac{1}{2}at\sin(t+\theta) \tag{1.1.1.8}$$

So the complete solution looks like

$$\begin{aligned} x &= a\cos(t+\theta) + \epsilon[-at\cos(t+\theta)] \\ &+ \epsilon^2[\frac{1}{2}at^2\cos(t+\theta) + \frac{1}{2}at\sin(t+\theta)] \end{aligned} \tag{1.1.1.9}$$

From Eq.(1.1.1.9) we can see that at t goes to $O(\epsilon^{-1})$ the approximation doesn't hold good. The term ϵx_1 and ϵx_2 are not small compared to x_0 and ϵx_1 respectively. So for large t this straight forward expansion method fails to provide satisfactory results.

This discrepancy can be visualized by analyzing the direct solution of Eq.(1.1.1.1), which gives after considering the initial condition as $x(0) = 0$ and $\dot{x}(0) = 1$

$$x = a\exp(-\epsilon t)\cos(\sqrt{1-\epsilon^2}t + \theta) \tag{1.1.1.10}$$

where $a = (1-\epsilon^2)^{-\frac{1}{2}}$;we compare this solution with Eq.(1.1.1.9) by taking the perturbation parameter ϵ is small and expanding the exponential and the

cosine term as

$$\exp(-\epsilon t) = 1 - \epsilon t + \frac{1}{2}\epsilon^2 t^2 + O(\epsilon^3) + ... \qquad (1.1.1.11)$$

$$\cos(\sqrt{1-\epsilon^2}t + \theta) = \cos(t+\theta) + \frac{1}{2}\epsilon^2 t \sin(t+\theta) + ... \qquad (1.1.1.12)$$

It is evident that the scheme gives the agreeable outcomes for a fixed t and small ϵ, particularly for $\epsilon t << 1$. In any case, typically we are intrigued for fixed ϵ, not t.In that case it is clearly observable from Eq.(1.1.1.12 and 1.1.1.12) that the comparison makes sense as long as $t << O(\epsilon^{-1})$. Ac-

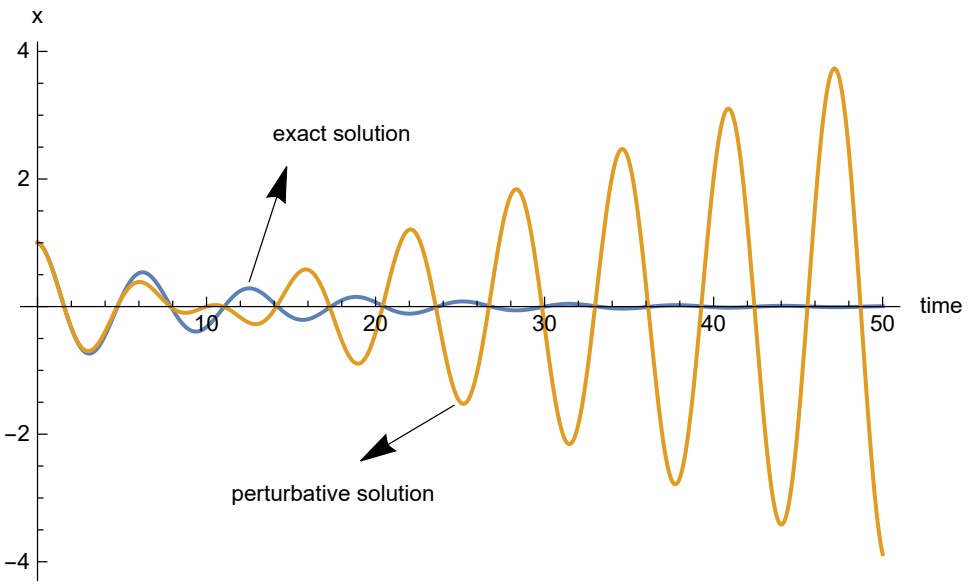

Figure 1.1: Plots of exact solution Eq.(1.1.1.10) and perturbative solution Eq.(1.1.1.9) with $\epsilon = 0.1$. As desired the perturbative series works fine upto $t << \epsilon^{-1} \sim 10$ and it differs after that.

cordingly to decide an extension substantial for times as large as ϵ^{-1},the combination ϵt ought to be viewed as a independent variable $T_1 = \epsilon t \sim O(1)$.

In particular this slow time scale T_1 will be regarded as constants on the fast time scale $T_0 = t$. Now the expansion Eq.(1.1.1.12) is valid for time as large as ϵ^{-1}. So that $\exp(-\epsilon t = \exp(-T_1))$. Similarly the expansion again breaks down as the time becomes comparable as $O(\epsilon^{-2})$. Also the frequency $\omega = \sqrt{1-\epsilon^2} \approx 1 - \frac{1}{2}\epsilon^2$ which is altered from $\omega = 1$, has a accumulative error for a large value of t, i.e. $t \sim \mathcal{O}(\epsilon^{-2})$. Then we have to consider again an independent time scale $T_2 = \epsilon^2 t$ which is slower than T_1. In brief we can suggest that, in order to evaluate the expansion valid for all t to the order of $\mathcal{O}(\epsilon^{-n})$ we have to find out the dependence of x on $(n+1)$ different time scales ,i.e. $T_0, T_1, ...T_n$, where

$$T_n = \epsilon^n t \tag{1.1.1.13}$$

In this way we can assume that,

$$\begin{aligned} x(t;\epsilon) &= x_0(T_0, T_1, T_2, ...) + \epsilon x_1(T_0, T_1, T_2, ...) \\ &+ \epsilon x_2(T_0, T_1, T_2, ...) + \mathcal{O}(\epsilon^3) \end{aligned} \tag{1.1.1.14}$$

Now using derivative expansion method [66],

$$\frac{d}{dt} = \frac{\partial}{\partial T_0} + \epsilon \frac{\partial}{\partial T_1} + \mathcal{O}(\epsilon^2) \tag{1.1.1.15}$$

$$\frac{d^2}{dt^2} = \frac{\partial^2}{\partial T_0^2} + 2\epsilon \frac{\partial^2}{\partial T_1 \partial T_0} + \mathcal{O}(\epsilon^2) \tag{1.1.1.16}$$

Now denoting the derivatives in subscript form for more compactness, the above two equations can be written as

$$\frac{d}{dt} = D_0 + \epsilon D_1 + \mathcal{O}(\epsilon^2) \tag{1.1.1.17}$$

$$\frac{d^2}{dt^2} = D_0^2 + 2\epsilon D_0 D_1 + \mathcal{O}(\epsilon^2) \tag{1.1.1.18}$$

where $D_n = \frac{\partial}{\partial T_n}$ Let us denote $\frac{dx}{dt} \equiv \dot{x}$ Then by Eq.(1.1.1.2) we can state by collecting powers upto $\mathcal{O}(\epsilon)$

$$\dot{x} = D_0 x_0 + \epsilon(D_1 x_0 + D_0 x_1) + \mathcal{O}(\epsilon^2) \tag{1.1.1.19}$$

and

$$\ddot{x} = D_0^2 x_0 + \epsilon(D_0^2 x_1 + 2D_0 D_1 x_0) + \mathcal{O}(\epsilon^2) \tag{1.1.1.20}$$

Now substituting above two equations into Eq.(1.1.1.2) and arranging the powers of ϵ accordingly

$$\mathcal{O}(1): \qquad D_0^2 x_0 + x_0 = 0 \tag{1.1.1.21}$$

$$\mathcal{O}(\epsilon): D_0^2 x_1 + x_1 = -2D_1 D_0 x_0 \tag{1.1.1.22}$$

Zeroth order solution yields

$$x_0 = a(T_1)\cos T_0 + b(T_1)\sin T_0 \tag{1.1.1.23}$$

Eq.(1.1.1.23) is a harmonic solution with its amplitude a and b are now function of *slow* time scale T_1 Now replace x_0 in Eq.(1.1.1.22) by Eq.(1.1.1.23) we can arrive at the differential equation for x_1,

$$\begin{aligned} D_0^2 x_1 + x_1 &= -2D_1 D_0(a(T_1)\cos T_0 + b(T_1)\sin T_0) \\ &= 2(a' + a)\sin T_0 - 2(b' + b)\cos T_0 \end{aligned} \tag{1.1.1.24}$$

where the prime denotes the differentiation with respect to the slow time T_1. Now the solution of x_1 gives *secular terms* which would bring us to a convergent but impractical series expansion of x. To get an approximation independent of secular terms we set the coefficients of the secular terms equal to zero, which yields

$$a' + a = 0 \tag{1.1.1.25}$$

$$b' + b = 0 \tag{1.1.1.26}$$

which lead to the solution

$$a(T_1) = a(0)\exp(-T_1) \tag{1.1.1.27}$$

$$b(T_1) = b(0)\exp(-T_1) \tag{1.1.1.28}$$

Now recalling the boundary conditions $x_0(0,0) = 0$ and $D_0 x_0(0,0) = 1$ give $a(T_1) = 0$ and $b(T_1) = 1$, so that

$$\begin{aligned} x_0 &= \exp(-T_1)\sin T_0 \\ &= \exp(-\epsilon T_0)\sin T_0 \\ &= \exp(-\epsilon t)\sin T_0 \end{aligned} \tag{1.1.1.29}$$

So the approximate solution is predicted by this method

$$x = \exp(-\epsilon t)\sin T_0 + \mathcal{O}(\epsilon) \tag{1.1.1.30}$$

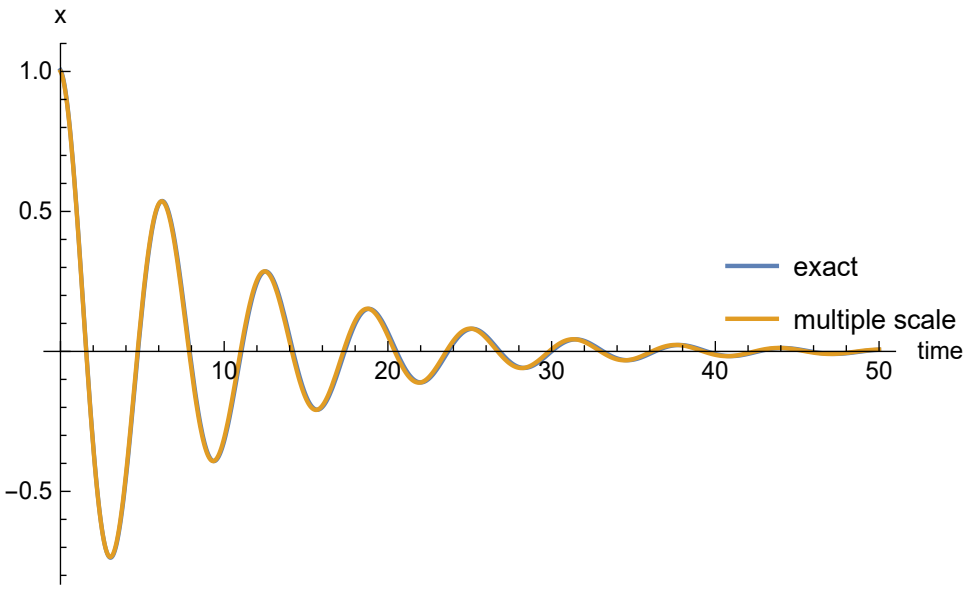

Figure 1.2: Plots of exact solution Eq.(1.1.1.10) and perturbative solution by multiple scale method Eq.(1.1.1.30) with $\epsilon = 0.1$.Two curves are almost indistinguishable.

One can go further by considering a more slower time $T_2 = \epsilon^2 t$ to examine the phase shift that occurred over a long time due to change in frequency as discussed earlier. So at this point, we have acknowledged how the multiple time scale framework functions. In the following section, we pick a more conventional nonlinear oscillator with cubic non-linearity, in writing known as Duffing Oscillator, and release the multiple scale technique to concentrate on its resonance response. The motivation to choose this particular oscillator is that, in the impending sections we will portray a few additional oscillators with parametric frequency, nonlinear damping, which will be changed in mix with this cubic non-linearity

1.1.2 Resonance in Duffing Oscillator: Application of multiple scale analysis

The Duffing oscillator has ended up a classical paradigm for outlining the remarkable jump wonder and other nonlinear conduct. The understanding picked up on the premise of this low-order nonlinear framework has made a difference in the improvement of reduced-order models of complex mechanical frameworks extending from micro-scales to macro-scales. A typical dimensionless forced duffing oscillator with damping is given as

$$\ddot{x} + \gamma\dot{x} + \omega_0^2 x + \alpha x^3 = f\cos\omega t \tag{1.1.2.1}$$

where $\gamma, \omega_0, \alpha, f$ are the damping constant, natural frequency, nonlinear stiffness, and the forcing amplitude respectively. The x^3 term added to the *damped harmonic oscillator* changes the scenario dramatically. We can not employ the superposition principle to deduce the resonance response, unlike simple oscillation. On the other hand the peak of resonance does not occur close to the natural frequency of the system; even the system in the presence of non-linearity can be phase-locked if the forced frequency is away from the natural frequency. Moreover the steady state response depends on the initial conditions in contrast to the linear oscillator whose response does not depend on the initial conditions. As (1.1.2.1) does not allow any closed form solution, the analytical approximation of forced response can be derived from the perturbation analysis. The *multiple scale perturbation* method is used as discussed previously in this and next few chapters.

Let introduce a perturbation parameter $\epsilon << 1$ an by assuming weak damping, weak nonlinerity, and weak forcing we can rewrite Eq.(1.1.2.1) as

$$\ddot{x} + \omega_0^2 x + \epsilon\tilde{\Gamma}\dot{x} + \epsilon\tilde{\Lambda}x^3 = \epsilon\tilde{F}\cos\omega t \tag{1.1.2.2}$$

where the scaled factors are $\gamma = \epsilon\tilde{\Gamma}, \alpha = \epsilon\tilde{\Lambda}, f = \epsilon\tilde{F}$. now by expanding x in straight forward two-time perturbative series to find out different possible

resonance

$$x(\tau_0, \tau_1) = x_0(\tau_0, \tau_1) + \epsilon x_1(\tau_0, \tau_1) + \epsilon^2 x_2(\tau_0, \tau_1) + ... \qquad (1.1.2.3)$$

Substituting Eq.(1.1.2.2) into Eq.(1.1.2.1) and collecting the terms order by order, and solving integro-differrential equations of corresponding orders of $\mathcal{O}(\epsilon)$ and $\mathcal{O}(\epsilon^2)$, it is noticed that secular terms appeared for $\omega \approx \omega_0$ at $\mathcal{O}(\epsilon)$ which is called *primary resonance*. Now unlike linear oscillator here secondary resonances appeared for $\omega \approx \frac{\omega_0}{3}$ and $\omega \approx 3\omega_0$ at the $\mathcal{O}(\epsilon^2)$. The first one is called *super harmonic* and the second is *sub harmonic* term respectively. We restrict our analysis to the primary resonance only to show that how the mechanism of multiple scale works for a nonlinear oscillator. Later we extend this method to more complicated oscillators involving parametric non linearity nonlinear damping etc.

Let us introduce a dimensionless time $\tau = \omega t$ and a detuning parameter $\tilde{\sigma}$ such that $\omega = \omega_0 + \epsilon\tilde{\sigma}$. Substituting these values into Eq.(1.1.2.2) we get,

$$x'' + x = -\epsilon\big[\Gamma x' + \Lambda x^3\big] + \epsilon F \cos\tau + \epsilon\sigma x \qquad (1.1.2.4)$$

where the prime denotes the derivative with respect to τ. The constants are given by $\Gamma = \frac{\tilde{\Gamma}}{\omega}, \Lambda = \frac{\tilde{\Lambda}}{\omega^2}, F = \frac{\tilde{F}}{\omega^2}$ and $\frac{\omega_0^2}{\omega^2} = 1 - \epsilon\sigma$ with $\sigma = \frac{2\epsilon\omega_0\tilde{\sigma}}{\omega^2}$. As discussed

in the previous section we can expand the derivatives as

$$\frac{d}{dt} = D_0 + \epsilon D_1 + \mathcal{O}(\epsilon^2) \tag{1.1.2.5}$$

$$\frac{d^2}{dt^2} = D_0^2 + 2\epsilon D_0 D_1 + \mathcal{O}(\epsilon^2) \tag{1.1.2.6}$$

where $D_n = \frac{\partial}{\partial \tau_n}$

Now using equation Eq.(1.1.2.3) to Eq.(1.1.2.4) and arranging the same power of ϵ we get the zeroth order $\mathcal{O}(\epsilon^0)$ solution as,

$$x_0 = a(\tau_1)\cos(\tau_0 + \phi(\tau_1)) \tag{1.1.2.7}$$

here we consider the amplitude and the phase are the functions of slow time τ_1. Equating both sides of Eq.(1.1.2.4) to the power of ϵ^1 we get the equation for x_1 as

$$
\begin{aligned}
D_0^2 x_1 + x_1 &= -2D_0 D_1 x_0 - \Gamma D_0 x_0 - \Lambda x_0^3 + F\cos\tau_0 + \sigma x_0 \\
&= 2[D_1 a \sin(\tau_0+\phi) + a\cos(\tau_0+\phi) D_1\phi] + \Gamma a \sin(\tau_0+\phi) \\
&- \Lambda a^3\Big[\frac{3}{4}\cos(\tau_0+\phi) + \frac{1}{4}\cos(3\tau_0+3\phi)\Big] + F\cos(\tau_0+\phi-\phi) \\
&+ \sigma a\cos(\tau_0+\phi) \\
&= 2[D_1 a \sin(\tau_0+\phi) + a\cos(\tau_0+\phi) D_1\phi] + \Gamma a \sin(\tau_0+\phi) \\
&- \Lambda a^3\Big[\frac{3}{4}\cos(\tau_0+\phi) + \frac{1}{4}\cos(3\tau_0+3\phi)\Big] + F\cos(\tau_0+\phi)\cos\phi \\
&+ F\sin(\tau_0+\phi)\sin\phi + \sigma a\cos(\tau_0+\phi) \qquad (1.1.2.8)
\end{aligned}
$$

At primary resonance all the secular terms give rise to unbounded solution of x_1; so that we equate all the coefficients of $\sin(\tau_0+\phi)$ and $\cos(\tau_0+\phi)$ term to zero which in turn delivers the flow equations, viz.

$$D_1 a = -\frac{1}{2}\Big[\Gamma a + F\sin\phi\Big] \qquad (1.1.2.9)$$

$$a D_1\phi = -\frac{1}{2}\Big[F\sin\phi + \sigma a - \frac{3\Lambda a^3}{4}\Big] \qquad (1.1.2.10)$$

The amplitude of equation is found around a fixed point(s) by setting $D_1 a_0 = D_1\phi_0 = 0$

$$\left(\Gamma a_0 + F\sin\phi_0\right)^2 + \left(F\cos\phi_0 + \sigma a_0 - \frac{3\Lambda a_0^3}{4}\right)^2 = 0 \qquad (1.1.2.11)$$

which gives a quadratics equation of σ whose solution is given by

$$\sigma = \frac{3}{4}\Lambda a_0^2 \pm \sqrt{\frac{F^2}{a_0^2} - \Gamma^2} \qquad (1.1.2.12)$$

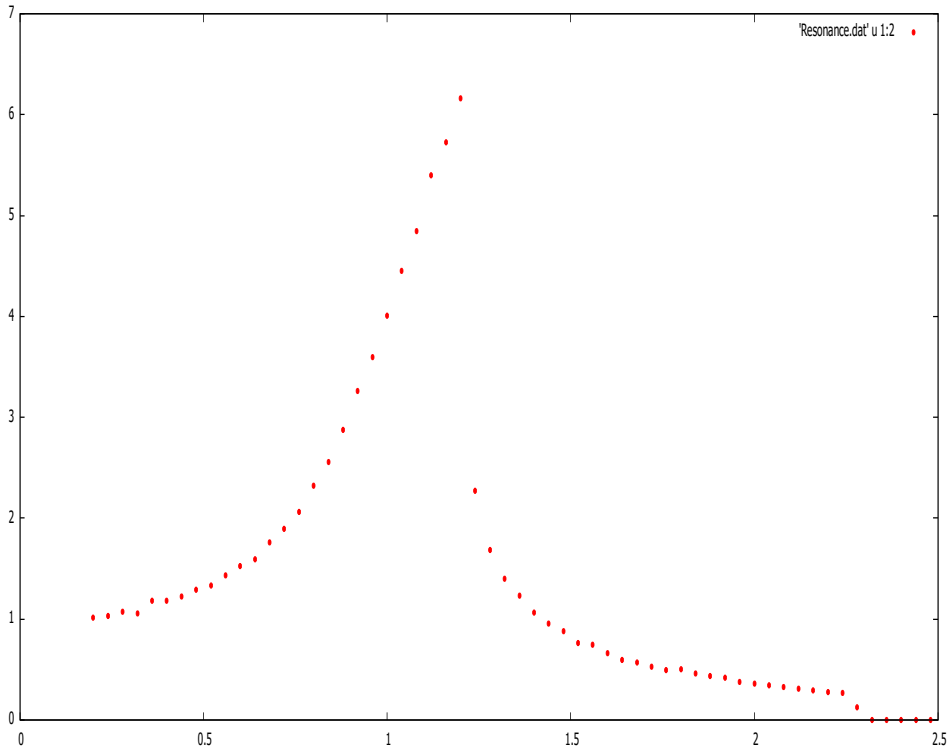

Figure 1.3: Resonance curve for duffing oscillator. With $\alpha = 2, \gamma = 0.1, \omega_0^2 = 1, f = 0.2$

Then by substituting this solution of σ into the relation $\frac{\omega_0^2}{\omega^2} = 1-\epsilon\sigma$ we get the analytical expression for amplitude frequency relation (frequency response curve) as

$$a_0 = \frac{4}{3\alpha}\sqrt{\omega^2 - \omega_0^2 \pm \sqrt{\frac{f^2}{a_0^2\omega^2} - \omega^2\gamma^2}} \tag{1.1.2.13}$$

This is the analytically derived amplitude response curve for duffing oscillator.In the next section we study a new kind of resonance which can only appear in the nonlinear systems.

1.2 Vibrational Resonance - A new practical approach as an applied theory of oscillations

The theory of vibrational structures and devices thinks about the normalities of excitation of vibration and its movement in various mechanical systems; it likewise incorporates the speculation of machines where vibration is valuable.In dislike of reality that actual oscillatory structures are nonlinear, various applied issues of the theory of mechanical movements can be particularly all around broke down in a straight setting of the issue, for example disregarding any nonlinear variables.

For decades the effects of external vibration on the linear system have been studied comprehensively, mainly focusing on the properties end effects of resonance. Regardless, to be certain those fairly principal commonalities have not at any rate been completely taken advantage of in vibrational design (not by any stretch like the electrical-or radio intending) ,to not communicate anything of nonlinear developments. The outcomes of the nonlinear systems are quite remarkable and diversified. Say, the vibration in a nonlinear system need not necessarily have to come from an external source, it may be an inherent quality of the system. We classify these kind of systems as parametric oscillators and discussed extensively in later chapters

The activity of vibration in nonlinear mechanical frameworks frequently leads to impossible to miss and now and then very startling comes about. These impacts, on the one hand, can be utilized in innovation, the standards of activity of very a number of most proficient machines being based on them, on the other hand, the same impacts may be the cause of undesirable and indeed lamentable circumstances. Effects of vibration can alter the behavior of the nonlinear oscillatory system. It can shift and change the characteristics of the equilibrium positions(i.e. stable or unstable equilibrium). It also affects the natural frequency of free oscillation. It the following chapters it will be also revealed that with the presence of nonlinear damping, vibration can effectively revise its value. One of the vital characteristics of the vibration is that it reforms dynamics of the system into an effective slow dynamics in contrast to the presence of the fast vibration, which is explained in detail in the next two sections.

1.2.1 A view through reference frames

A large portion of the counted impacts are portrayed by the way that the advancement which shows up in the framework under vibration can be introduced as a proportion of two areas; the *"rapid or fast"*, *"vibrational"* part, and the *"slow"* part which changes very little in one time of vibration, and the sluggish improvement is of surprising interest in far beyond anyone's expectations by far most of the cases. Grant us to envision that there is a passerby who doesn't have even the remotest clue (or needs to notice) either

those rapid (as a last resort, essentially nothing) advancements or fast forces. This spectator is either wearing magnificent glasses which don't allow him to see the quick advancements of the design, or he might be watching the improvement in the stroboscopic (for example infringed) light, the rehash of glimmers being similar to that of vibration. This spectator V, as opposed to the typical passerby O who "sees everything", will see essentially the apathetic piece of the turn of events, and if he ought to struggle with the laws of mechanics, he should sort out that tremendous number of huge impacts by the presence of express extra sleepy powers or minutes acting close by the standard drowsy powers. We will call them after Kapitsa [63, 64] "vibrational powers". As demonstrated by the perspective of that "lopsided" spectator, those powers cause the above impacts on which the particular use of vibration is based.

Let the equation is represented by the equation

$$\mathbf{m\ddot{x}} = \mathbf{F}(\dot{\mathbf{x}}, \mathbf{x}, \mathbf{t}) + \mathbf{V}(\dot{\mathbf{x}}, \mathbf{x}, \mathbf{t}, \mathbf{\Omega t})$$

where F is the *slow* force and V is the *fast or vibrational* force. The fast force not only depends on t but also has an explicit dependence on the vibrational frequency $\Omega >> \omega$. Let us assume (will be clarified in the next section) the motion of the system is described by

$$\mathbf{x} = \mathbf{s}(\mathbf{t}) + \mathbf{f}(\mathbf{t}, \mathbf{\Omega t})$$

here s and f are the *slow* and *fast* components of motion respectively. Then the observer V who doesn't see the fast force or fast component, to him the effective motion will appear as

$$\mathbf{m\ddot{s}} = \mathbf{F}(\mathbf{s}, \dot{\mathbf{s}}, \mathbf{t}) + \mathbf{F_v}(\mathbf{s}, \dot{\mathbf{s}}, \mathbf{t})$$

where F is the slow force and F_v may be introduced as *pseudo forces* widely known as *vibrational forces* in the study of vibrational mechanics. Subsequently, we come to the assertion, in many regards like the notable hypothesis of the mechanics of relative movement. As indicated by that hypothesis, the eyewitness, associated with the direction framework moving with the speed increase, should add the forces of inertia to every one of the conventional forces applied to the reference frame.

For our circumstance, the onlooker V who doesn't see either the speedy forces or the fast developments ought to add vibrational forces to each standard force. While in the mechanics of relative motion we add pseudo forces (forces of inertia) to each standard force of the dynamics under concern for the use of the non-inertial (for instance moving with speed increment) coordinate system, for our circumstance the extension of vibrational forces is a fine for the ignoring the fast (ordinarily small) developments of the structure.

On this record, the mechanics by which the onlooker V is facilitated (the spectator who sees no fast drives or rapid turns of events) will be called by us ***vibrational mechanics.***

We can schematically depict the above argumentation in the figure (1.4).

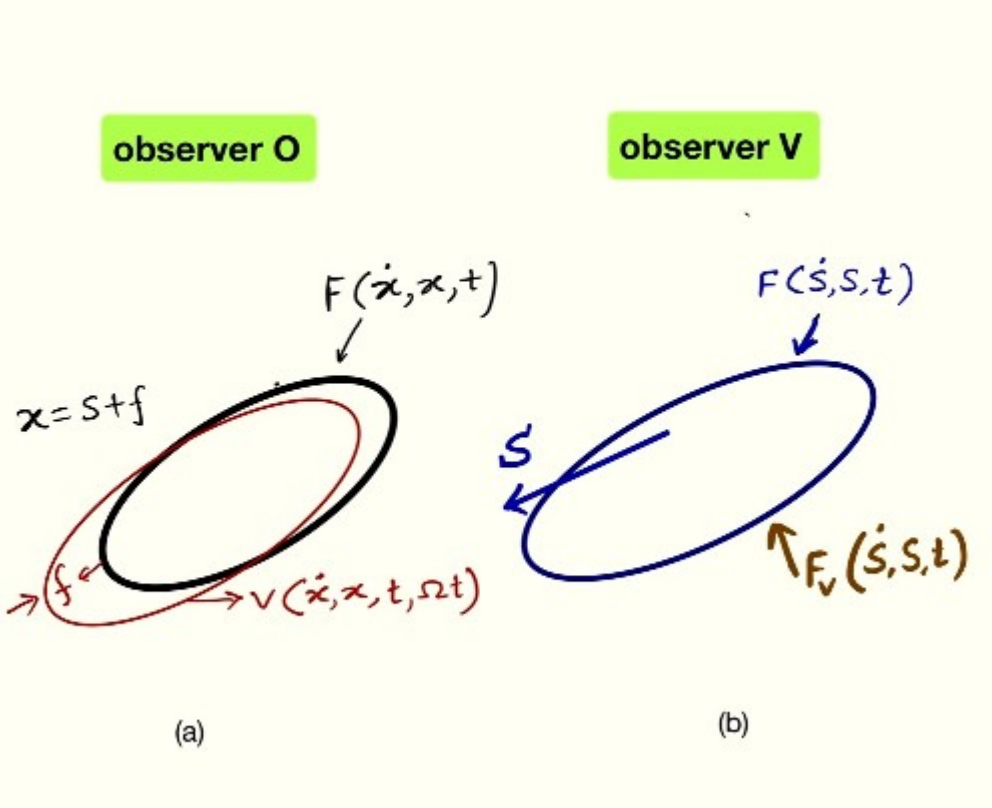

Figure 1.4: (a): The dynamics seen by observer **O** (b): The dynamics seen by the observer **V**

Left hand side of the figure describes how the observer **O** perceives the motion, i.e. he notices all the components of motion namely *slow, s* and *fast, f* simultaneously. In contrast the observer V only detects the effective *slow* motion along with a vibrational force F_v.

1.2.2 Mathematical tools of vibrational resonance: Direct partition of motion

A plethora of events and action in natural science and engineering taking place under the influence of vibration. In non-linear frameworks the dynamics under the impression of such vibration can be characterized by a dual impact of "fast" and "slow" motions. Our sole purpose is to study the this slow dynamics.In vibrational resonance it the effective slow motion of the nonlinear system which maximizes its response by suitably controlling the fast forcing drive.

We now discuss the procedure to operate these forces by means of *Direct Partition of Motion* [12]. This method involves two stages. At first the initial system of motion(differential equation) with hidden components(fast or vibrational components) is converted into an integro-differential equation by selecting a particular form of fast forcing. Then at the second stage an approximate solution is obtained by assuming the dynamic variable consists of a *slow* and a *fast* variable due to difference in the regarding time scales.

Let us first start with a system under consideration which can be presented in the following form

$$\mathbf{m\ddot{x}} = \mathbf{F}(\dot{\mathbf{x}}, \mathbf{x}, \mathbf{t}) + \mathbf{V}(\dot{\mathbf{x}}, \mathbf{x}, \mathbf{t}, \mathbf{\Omega t}) \tag{1.2.2.1}$$

m denotes the mass, **F** and **V** are n-dimensional vector forces. From now these are designated as slow and fast forces respectively. For the purpose of the thesis we restrained ourselves to 1-dimensional cases, so that **F** and **V** can be treated as scalar only. Ω is assumed to be large in comparison to the characteristics slow frequency of the system. To say, the term *'large'* is to be justified mathematically shortly. Vibrational force **V** is supposed to nearly 2π periodic in time $\tau = \Omega t$. τ is called the *fast time* and t as *slow or frozen time.*

Now as described in the previous paragraph we can assume

$$x(t, \tau) = s(t) + f(t, \tau) \tag{1.2.2.2}$$

here s and f are the slow and fast components of the generalized coordinate of motion. We will assume that f is periodic in time τ, so that

$$\left\langle f \right\rangle = \frac{1}{2\pi} \int_0^{2\pi} f(t, \tau) d\tau = 0. \tag{1.2.2.3}$$

Now substituting Eq.(1.2.2.2) into Eq.(1.2.2.1) we arrive at the pair of equation describing two integro-differential equations of slow and fast motion separately, viz.

$$m\ddot{s} = F(\dot{s}, s, t) + \left\langle \tilde{F}(\dot{s}, \dot{f}, s, f, t) \right\rangle + \left\langle V(\dot{s} + \dot{f} + s + f, t, \tau) \right\rangle. \quad (1.2.2.4)$$

and

$$\begin{aligned} m\ddot{f} &= \tilde{F}(\dot{s}, \dot{f}, s, f, t) + V(\dot{s} + \dot{f} + s + f, t, \tau) \\ &- \left\langle \tilde{F}(\dot{s}, \dot{f}, s, f, t) \right\rangle - \left\langle V(\dot{s} + \dot{f} + s + f, t, \tau) \right\rangle \end{aligned} \quad (1.2.2.5)$$

where the function

$$\tilde{F}(\dot{s}, \dot{f}, s, f, t) \rangle = F(\dot{s} + \dot{f}, s + f, t) - F(\dot{s}, s, t) \quad (1.2.2.6)$$

is zero when $\dot{f} = 0$ and $f = 0$

We can argue that the splitting of Eq.(1.2.2.1) into these equivalent Eqs. (1.2.2.4) and (1.2.2.5) makes sense in way that if s and f have some particular solution which satisfy the aforementioned equations, then $x = s + f$ is also a solution of Eq.1.2.2.1. In other words if there exists a solution of x of type Eq.(1.2.2.2) then it is adequate that there ought to be a corresponding

solution of s and f.

Vibrational Motion: Assumptions, Formalizations, and Conditions of its fulfillment

Here we justify the reason behind the assumption that Eq.(1.2.2.1) has the solution of type Eq.(1.2.2.2). Let us now examine why the terms s and f are called "*slow*" and "*fast*" by giving mathematical validity to this whole framework.

To investigate this let us first define the scale of s and f by s_0 and f_0 in such way that

$$\frac{s}{s_0} \sim \mathcal{O}(1) \;\; and \;\; \frac{f}{f_0} \sim \mathcal{O}(1) \tag{1.2.2.7}$$

Let assume f changes to the order of f_0 in shortest period of time T and s vary slowly with respect to f, provided that the following condition is satisfied.

$$\frac{s|_{t+T} - s|_t}{s_0 T} : \frac{f|_{t+T} - f|_t}{f_0 T} \approx \frac{\dot{s}}{s_0 T} : \frac{\dot{f}}{f_0 T} \sim \epsilon \tag{1.2.2.8}$$

Eq.(1.2.2.7) expresses the fact that the variable s changing with relative

speed of the order ϵ with respect to the relative speed of changing f, ϵ being a small parameter. As $f = f(t, \Omega t)$, by using total derivative of f Eq.(1.2.2.8) becomes

$$\frac{\dot{s}}{s_0 T} : \frac{\dot{f}}{f_0 T} = \frac{1}{s_0}\frac{ds}{dt} / \frac{1}{f_0}(\frac{\partial f}{\partial t} + \Omega \frac{\partial f}{\partial \tau}) \sim \epsilon \tag{1.2.2.9}$$

Consequently it very well may be seen that for the legitimacy of the supposition about the pace of changing the components s and f, it is adequate (in spite of the fact that not essential!) to recognize the small parameter ϵ with the worth $\frac{1}{\Omega}$ and urging that $\frac{1}{s_0}\frac{ds}{dt}$ and $\frac{1}{f_0}\frac{\partial f}{d\tau}$ are of the same order and $\frac{1}{f_0}\frac{\partial f}{\partial t}$ be of same of higher order with respect to $\epsilon = \frac{1}{\Omega}$ it may be in particular $\frac{1}{f_0}\frac{\partial f}{\partial t} \equiv 0$, then we can state that

$$\frac{\dot{s}}{\dot{f}}\frac{f_0}{s_0} \sim \epsilon = \frac{1}{\Omega} \tag{1.2.2.10}$$

So we can conclude our above discussions in the following statement as

$$\begin{gathered} \Omega = \frac{1}{\epsilon} >> 1, \\ \mathcal{O}(\frac{1}{s_0}\frac{ds}{dt}) = \mathcal{O}(\frac{1}{f_0}\frac{\partial f}{d\tau}), \quad \mathcal{O}(\frac{1}{f_0}\frac{\partial f}{\partial t}) \geq \mathcal{O}(\frac{1}{f_0}\frac{\partial f}{d\tau}) \end{gathered} \tag{1.2.2.11}$$

the above conditions are sufficient for the validity of the main assumptions

of vibrational mechanics

The easiest illustration of the sets of capacities s and f, fulfilling condition Eq.(1.2.2.11) is given by $s = s_0 \sin t$ and $f = f_0 \sin \Omega t$.In this association we should underline that condition Eq.(1.2.2.11) and, thusly, the primary supposition of vibrational mechanics, as it was formed above, doesn't force any limitation on the proportion of the outright upsides of the components s and f.The value f_0 isn't fundamentally little in comparison to s_0, it may be comparable to s_0 and indeed bigger than that. In other words, the sufficiency of the vibration of high-frequency f_0 can be of the same order or indeed much bigger than the scale of alter of the moderate component.

Now in same way we can write as Eq.(1.2.2.9)

$$\frac{\ddot{s}}{s_0 T^2} : \frac{\ddot{f}}{f_0 T^2} = \frac{1}{s_0}\frac{d^2 s}{dt^2} / \frac{1}{f_0}(\frac{\partial^2 f}{\partial t^2} + 2\Omega \frac{\partial^2 f}{\partial t \partial \tau} + \Omega^2 \frac{\partial^2 f}{\partial \tau^2}) \sim \epsilon^2 \quad (1.2.2.12)$$

by also believing the following conditions should be satisfied,

$$\mathcal{O}(\frac{1}{s_0}\frac{d^2 s}{dt^2}) = \mathcal{O}(\frac{1}{f_0}\frac{\partial^2 f}{d\tau^2}), \quad \mathcal{O}(\frac{1}{f_0}\frac{\partial^2 f}{\partial t^2}, \frac{\epsilon}{f_0}\frac{\partial^2 f}{\partial t \partial \tau}) \geq \mathcal{O}(\frac{1}{f_0}\frac{\partial^2 f}{d\tau^2}) \quad (1.2.2.13)$$

finally we arrive at the conclusion

$$\frac{\ddot{s}}{\ddot{f}}\frac{f_0}{s_0} \sim \epsilon^2 = \frac{1}{\Omega^2} \tag{1.2.2.14}$$

Now by comparing Eq.(1.2.2.10) and Eq.(1.2.2.14) it can be formulated that if,

$$\frac{f_0}{s_0} \sim \epsilon^m, \quad m = ..., -1, 0, 1, 2.... \tag{1.2.2.15}$$

i.e. the fast component is of order m of the slow component s, then

$$\frac{\dot{s}}{\dot{f}} \sim \epsilon^{1-m}, \qquad \frac{\ddot{s}}{\ddot{f}} \sim \epsilon^{2-m} \tag{1.2.2.16}$$

So now by comparing Eq.(1.2.2.16) with Eq.(1.2.2.4) and Eq.(1.2.2.5) we can wrap up by stating that for the validity of the main assumption it is necessary that the right hand side of Eq.(1.2.2.5) should be order of ϵ^{m-2} if the right hand side of Eq.(1.2.2.4) is taken of the $\mathcal{O}(1)$. In conclusion, this can be summarized as

$$m\ddot{s} = M; \qquad m\ddot{f} = \frac{N}{\epsilon^{2-m}} \tag{1.2.2.17}$$

where M and N are given as

$$M = F+ < \tilde{F} > + < V > \quad and \quad N = \tilde{F}- < \tilde{F} > +V- < V > \tag{1.2.2.18}$$

with $|M|$ and $|N|$ are of the same order.

Application to Duffing oscillator

We now proceed further to show that how the above formalism can be applied to a simple nonlinear system. We consider a under damped *Duffing Oscillator* as the model for analysis, viz.

$$\ddot{x} + \gamma\dot{x} + \omega_0^2 x + \alpha x^3 = c\cos(\omega t) + g\cos(\Omega t) \tag{1.2.2.19}$$

We can think of the motion of the particle in a mono stable potential, viz.

$$V(x) = \frac{1}{2}\omega_0^2 x + \frac{1}{4}\alpha x^4 \tag{1.2.2.20}$$

Depending on the sign of ω_0^2 and α we can introduce four types of potential

1. For $\omega_0^2 > 0$ and $\alpha > 0$, it is a mono-stable or single well potential with minimum at $x = 0$.

2. For $\omega_0^2 < 0$ and $\alpha > 0$, we say the potential is double-well or bi-stable one with two minima at $x = \pm\sqrt{\frac{|\omega_0^2|}{\alpha}}$ and a maxima at $x = 0$.

3. For $\omega_0^2 > 0$ and $\alpha < 0$, it a double hump potential with minima at $x = 0$ and two maxima at $x = \pm\sqrt{\frac{|\omega_0^2|}{\alpha}}$.

4. Finally for both $\omega_0^2, \alpha < 0$, we have an inverted potential with maxima at $x = 0$

Now dividing x into slow and fast component as done in Eq.(1.2.2.2) and writing the equations of slow and fast dynamics separately,

$$\ddot{s} + \gamma\dot{s} + \omega_0^2 s + 3\alpha s^2\langle f\rangle + 3\alpha s\langle f^2\rangle + \langle f^3\rangle = c\cos(\omega t) \tag{1.2.2.21}$$

$$\ddot{f} + \gamma\dot{f} + \omega_0^2 f + 3\alpha s^2(f - \langle f\rangle) + 3\alpha s(f^2 - \langle f^2\rangle) + (f^3 - \langle f^3\rangle) = g\cos(\Omega t) \tag{1.2.2.22}$$

where

$$\langle f^p\rangle = \frac{1}{2\pi}\int_0^{2\pi} f^p d(\Omega t) = 0 \tag{1.2.2.23}$$

Hence applying the *inertial approximation* Eq.(1.2.2.13) we argue that $\ddot{f} >> \dot{f} >> f^2, f^3, f$ such that Eq.(1.2.2.22) modified to

$$\ddot{f} = g\cos(\Omega t)$$
$$\implies f = -\frac{g}{\Omega^2}\cos(\Omega t) \tag{1.2.2.24}$$

So by Eq.(1.2.2.22)

$$\langle f^2 \rangle = \frac{g^2}{2\Omega^4} \quad and \quad \langle f^3 \rangle = 0 \tag{1.2.2.25}$$

Substituting these values Eq.(1.2.2.20) we declare the equation for slow motion

$$\ddot{s} + \gamma\dot{s} + \tilde{\omega}^2 s + \alpha s^3 = c\cos(\omega t) \tag{1.2.2.26}$$

This equation can be stated as the motion of a system under an effective potential

$$V_{eff} = \frac{1}{2}\tilde{\omega}^2 s + \frac{1}{4}\alpha s^4 \tag{1.2.2.27}$$

where the effective natural frequency of the system becomes

$$\tilde{\omega}^2 = \omega^2 + \frac{3\alpha g^2}{2\Omega^4} \tag{1.2.2.28}$$

It is clearly visible from Eq.(1.2.2.27) that the shape of the effective potential

can be controlled by tuning the fast forcing parameter g and Ω. Consequently, by manipulating these terms one can change the equilibrium states. Here, in this section, our discussion is confined to single well potential only, which is physically pertinent and easy to realize. In the upcoming chapters we engage ourselves with more complex potentials with multiple extrema and time dependency.

Let the equilibrium point of Eq.(1.2.2.27) is $s* \neq 0$ about which oscillation happens. By changing the $u = s - s*$ and substituting it into Eq.(1.2.2.26) and neglecting the nonlinear terms, we can give an analytical solution for $c << 1$ and long time limit $t \to \infty$ as

$$u = Q_L \cos(\omega t + \delta) \tag{1.2.2.29}$$

where the amplitude and the phase given by

$$Q_L = \frac{c}{\sqrt{(\tilde{\omega}^2 - \omega^2)^2 + \gamma^2\omega^2}} \quad and \quad \delta = \tan^{-1}\left(\frac{\gamma\omega}{\omega^2 - \tilde{\omega}^2}\right) \tag{1.2.2.30}$$

Eq.(1.2.2.31) provides the analytical expression for vibrational amplitude, where the response the oscillator can be visualized by tuning the parameter g. In contrast to the conventional resonance where the amplitude is varied as a function of the forcing frequency ω. This is one of the exclusive features of vibrational resonance. We now discuss the numerical algorithm to support

this analytical prediction [10]. Numerically Q_L is given by

$$Q_L = \frac{\sqrt{Q_s^2 + Q_c^2}}{c} \tag{1.2.2.31}$$

where

$$Q_s(\omega) = \frac{2}{nT}\int_0^{nT} x(t)\sin(\omega t)dt \tag{1.2.2.32}$$

$$Q_c(\omega) = \frac{2}{nT}\int_0^{nT} x(t)\cos(\omega t)dt. \tag{1.2.2.33}$$

We plot the analytical and numerical results in the following figure (1.5).

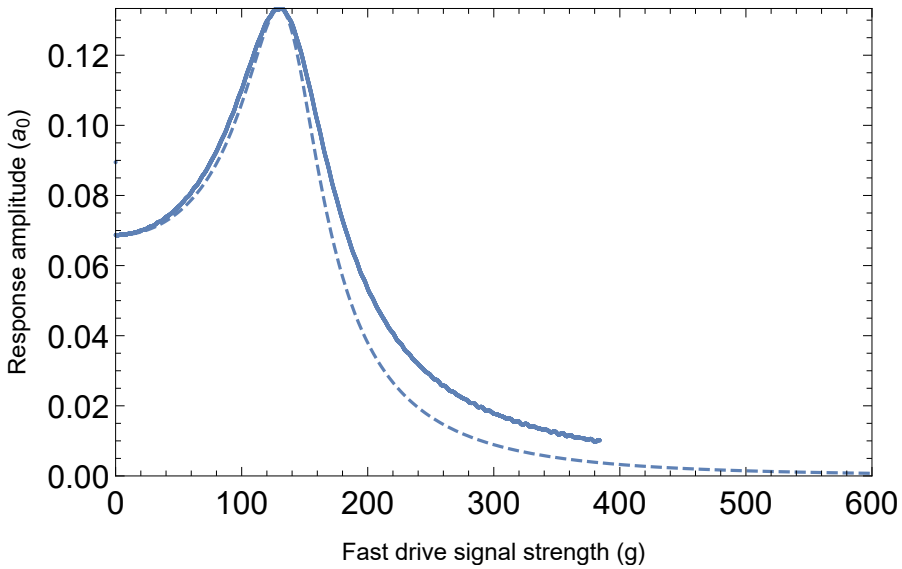

Figure 1.5: Dashed line represents analytical (Eq.1.2.2.31) plot and the solid line represents numerical (Eq.1.2.2.32) plot. Parameters are taken as $\omega_0^2 = 1$,$\Omega = 15$,$\omega = 1.5$, $\gamma = 0.5$ and $\alpha = 1$

Now we arrive at a point to discuss the importance of non-linearity of to

study the effects of vibrational resonance. One might ask that : is there any effect of fast forcing on a linear system? Or, can one get the vibrational response in a linear system? The answer is straight forward and can be perceived by the solution of the Eq.(1.2.2.19) without the nonlinear term, i.e $\alpha = 0$. We can write down the solution as

$$x(t) = Q_1 e^{p_1 t} + Q_2 e^{p_2 t} + Q_\omega \cos(\omega t + \phi_1) + Q_\Omega \cos(\Omega t + \phi_2) \quad (1.2.2.34)$$

where

$$p_{1,2} = \frac{1}{2}(-\gamma \pm \sqrt{\gamma^2 - 4\omega_0^2}) \quad (1.2.2.35)$$

$$Q_\omega = \frac{c}{\sqrt{(\omega_0^2 - \omega^2)^2 + \gamma^2\omega^2}} \quad , \quad Q_\Omega = \frac{g}{\sqrt{(\omega_0^2 - \Omega^2)^2 + \gamma^2\Omega^2}} \quad (1.2.2.36)$$

Q_1 and Q_2 are determined by the initial conditions. For $t \to \infty$ the first two transient terms go off to zero. So the solution essentially consist of two periodic terms for long time limit. It is to be noticed that the slow frequency amplitude Q_ω is uninfluenced by the parameters of fast forcing g and Ω. It can be only controlled by the slow drive strength c on a linear system. So we deduce that one can not discuss vibrational resonance in a linear system system.

Chapter 2

Vibrational Response of a Mathieu-Duffing Oscillator in the Presence of Slow and Fast Drive Simultaneously

- **Motivation of this chapter**

  Studies on enhanced response of a trapped system to a low frequency field as a consequence of the presence of some rapidly varying excitation has been a subject of extensive investigation during the last four decades. The excitation can be either of a random nature represented by some additive or multiplicative noise, or of a deterministic nature

realizable by a high frequency periodic forcing. In the former case, the widely addressed field of stochastic resonance has played a central role in revealing interesting physics of bistable[1, 2], monostable [3, 4] and excitable[5, 6] classical as well as quantum [7, 8] systems. In the latter case, the phenomenon of vibrational resonance gained prominence from the work of Landa and McClintock [10] following which theoretical[11, 12],numerical [13] as well as experimental [14, 15] works with special emphasis on nonlinear systems [16, 17, 18, 19, 20, 21, 22, 23, 24, 25] have been extensively pursued.

Among a wide variety of nonlinear systems, those with parametric excitations have been an important subject of study ever since Michael Faraday observed – as early as in 1831 – that the surface wave of a fluid filled cylinder, excited vertically, had the time period twice that of its own natural oscillation. Since then a plethora of work encompassing all disciplines of natural sciences as well as engineering have been carried out [26, 27, 28, 29, 30, 31, 32, 33]. The response, stable or unstable, of a system subjected to parametric excitation is sensitively dependent on the values of the parameters involved and endeavors for proper understanding of the stability characteristics of such oscillators have led to developments of rich methods in perturbation theory and dynamical systems in general.

However, it appears that apart from a few recent works [34, 35, 36, 37],

investigations of the behavior of parametric oscillators in the backdrop of vibrational resonance have not been that extensive. In this chapter we study a parametric bistable oscillator subjected to a combination of slow and rapid frequency forcing and find out, using perturbation theory, how the system responds nonlinearly to the slow drive as one varies the strength of the fast-frequency excitation. The layout of this chapter as follows:- In Sec.**2.1** we describe the model and the rationale behind its consideration. In Sec.**2.2** we go into detailed mathematical considerations followed by numerical simulations in Sec.**2.3**. Satisfactory agreement is observed between the analytical and numerical results. The is concluded in Sec.**2.4**.

2.1 Description of the model

The oscillator we shall study in this chapter has three forcing functions operative simultaneously. The setting of a typical problem pertaining to the phenomenon of vibrational resonance, as has been alluded to in the Introduction, has two forcing frequencies at play where one is much larger in magnitude than the other. Usually, the role of the higher forcing frequency is to catalyse the resonant response of the system to the lower forcing frequency over wider ranges. These frequencies are considered in a different footing from the natural frequency of the oscillator. The objective of the present chapter is to bring in a periodic variation in the natural frequency

of the oscillator with a frequency that coincides with the lower forcing frequency just mentioned above. The equation of such a parametrically driven oscillator looks like

$$\ddot{x} + \gamma\dot{x} - \omega_0^2(1 + q\cos\omega_p t)x + \alpha x^3 = c\cos\omega t + g\cos\Omega t \tag{2.1.1}$$

where $c\cos\omega t$ is the term denoting the lower frequency drive while $g\cos\Omega t$ represents the higher frequency drive and, as stated above, the parametric frequency ω_p is equal to the lower forcing frequency, viz.,

$$\omega_p = \omega. \tag{2.1.2}$$

The minus sign before ω_0^2 in Eq.(2.1.1) signifies that the oscillator is sitting on the apex of the barrier separating two wells and hence is ideally unstable, provided, that the periodic function $(1+q\cos\omega_p t)$ remains positive and hence we would require that the range of the dimensionless parameter q should be $-1 < q < 1$. It is a well studied fact that, without the parametric term ($q = 0$), the role of the high frequency term $g\cos\Omega t$ is, primarily, to stabilize the system by redressing the natural frequency term in such a way that effectively it looks like a naive Duffing oscillator subjected to the lower frequency forcing only.

When the parametric drive is present ($q \neq 0$) then the high frequency term

($g\cos\Omega t$) has an additional role to play. To first order in perturbation theory, where predictions made by the amplitude and phase equations for a forced Duffing oscillator almost exactly match with numerical simulations [65, 67], we shall show that without the high frequency drive the parametric term is not visible to the system at all, i.e., with $g = 0$, the variables q and ω_p do not participate in the flow equations. But with the inclusion of the high frequency drive the presence of the parametric drive is felt in that the parameters q and ω_p get mixed up in a way as to give rise to an effective frequency that now responds resonantly to the low frequency drive term denoted by $c\cos\omega t$. Keeping this fact in mind we shall, for the first part of the following calculations, pretend that ω_p and ω are two different frequencies although, for this chapter, they are actually not. The sole objective behind this difference in denotation is to point out that, despite they being same, it is the frequency of the parametric drive that is functional in producing the effective frequency.

2.2 Analytical expression for response amplitude

We divide this Section into two parts, the first one describing how the parametric and the fast frequency drives combine to produce an effective frequency and the second one focuses on the flow equations.

The effective frequency

Owing to the presence of two different driving frequencies we expect that the system's response can also be split up into two distinct time scales, one slow and the other fast, and accordingly we can write the dynamical variable of Eq.(2.2.1) as a sum of a slow variable $s \equiv s(t, \omega t)$ and a fast variable $f \equiv f(t, \Omega t)$, viz.,

$$x(t) = s(t, \omega t) + f(t, \Omega t). \tag{2.2.1}$$

The time period of oscillation of the slow variable ($= 2\pi/\omega$) being much larger than the time period of the fast variable ($= 2\pi/\Omega$), the average of the fast variable over a full time period is zero, i.e., with $\tau = \Omega t$,

$$\langle f(t, \tau) \rangle = \frac{1}{2\pi} \int_0^{2\pi} f(t, \tau) d\tau = 0. \tag{2.2.2}$$

This, along with the property that the derivative(s) of a fast variable are much larger in magnitude than the variable itself (i.e., $\ddot{f} \sim \dot{f} \gg f, f^2, f^3$), allow us to split Eq.(2.2.1) into the following two equations:

$$\ddot{s} + \gamma \dot{s} - s F_0(t) + \alpha F_1(s, f) = c \cos \omega t \tag{2.2.3}$$

$$\ddot{f} + \gamma \dot{f} - f F_0(t) + \alpha F_2(s, f) = g \cos \Omega t \tag{2.2.4}$$

where, the parametrically oscillating function $F_0(t)$ is given by

$$F_0(t) = \omega_0^2(1 + q\cos\omega_p t), \tag{2.2.5}$$

and the functions associated with the strength of nonlinearity α are given by

$$\begin{aligned} F_1(s,f) &= s^3 + 3s^2\langle f\rangle + 3s\langle f^2\rangle + \langle f^3\rangle & (2.2.6)\\ F_2(s,f) &= 3s^2(f - \langle f\rangle) + 3s(f^2 - \langle f^2\rangle) \\ &+ (f^3 - \langle f^3\rangle). & (2.2.7) \end{aligned}$$

In Eq.(2.2.4) the αF_2 term being much smaller than the other ones, we neglect it and proceed to solve the remaining equation self-consistently [by first putting off the parametrically oscillating term, solving the remaining equation and finally re-invoking this term] to obtain the equation

$$\begin{aligned} \ddot{f} + \gamma\dot{f} &= gB\cos(\Omega t + \phi) \\ &+ gQ[\cos(\chi t + \beta) + \cos(\xi t + \beta)] & (2.2.8) \end{aligned}$$

where the newly brought in frequencies are

$$\chi = \Omega + \omega_p \tag{2.2.9}$$

$$\xi = \Omega + \omega_p, \tag{2.2.10}$$

the newly brought in dimensionless amplitude factors are

$$B = \sqrt{(1 + A\cos\beta)^2 + (A\sin\beta)^2} \tag{2.2.11}$$

$$Q = \frac{qA}{2} \tag{2.2.12}$$

with A, also dimensionless, given as

$$A = \frac{\omega_0^2}{\Omega\sqrt{\Omega^2 + \gamma^2}}, \tag{2.2.13}$$

and the newly brought in phase terms are

$$\beta = \tan^{-1}\left(\frac{\gamma}{\Omega}\right) \tag{2.2.14}$$

$$\phi = \tan^{-1}\left(\frac{A\sin\beta}{1 + A\cos\beta}\right). \tag{2.2.15}$$

With three periodic forcing terms sitting on the right hand side of Eq.(2.2.8),

its solution evaluates to

$$\begin{aligned} f(t) &= \frac{g}{\mu_1}\cos(\Omega t+\phi+\theta)+\frac{g}{\mu_2}\cos(\chi t+\beta+\delta) \\ &+ \frac{g}{\mu_3}\cos(\xi t+\beta+\nu) \end{aligned} \tag{2.2.16}$$

where the additional phase terms are given by

$$\theta = \tan^{-1}\left(\frac{\gamma}{\Omega}\right) \tag{2.2.17}$$

$$\delta = \tan^{-1}\left(\frac{\gamma}{\chi}\right) \tag{2.2.18}$$

$$\nu = \tan^{-1}\left(\frac{\gamma}{\xi}\right) \tag{2.2.19}$$

and the μ's sitting in the amplitudes on the right hand side of Eq.(2.2.16) are given by

$$\mu_1 = \frac{\Omega^2(\Omega^2+\gamma^2)}{\sqrt{(\Omega^2-\omega_0^2)^2+\Omega^2\gamma^2}} \tag{2.2.20}$$

$$\mu_2 = \frac{2\chi\Omega\sqrt{(\gamma^2+\chi^2)(\gamma^2+\Omega^2)}}{q\omega_0^2} \tag{2.2.21}$$

$$\mu_3 = \frac{2\xi\Omega\sqrt{(\gamma^2+\xi^2)(\gamma^2+\Omega^2)}}{q\omega_0^2}. \tag{2.2.22}$$

The high-frequency periodic functions constituting the form of $f(t)$ in Eq.(2.2.16) confirm that the average of $f(t)$ over a complete time period is zero in accordance with Eq.(2.2.2). It also follows from Eqs.(2.2.20)-(2.2.22) that since Ω is large, the magnitudes of the μ_i's are of the order of Ω^2, thus resulting in the amplitudes of the high-frequency terms in Eq.(2.2.16) to take small values which, in retrospect, rationalizes the self-consistent technique we have adopted above in order to arrive at Eq.(2.2.8). From Eq.(2.2.16) it further follows that the averages of the square and cube of $f(t)$ are

$$\langle f^2 \rangle = \frac{g^2}{2} \sum_{i=1}^{3} \frac{1}{\mu_i^2} \tag{2.2.23}$$

$$\langle f^3 \rangle = 0. \tag{2.2.24}$$

The values of the averages of the first, second and third powers of $f(t)$ given respectively by Eqs.(2.2.2), (2.2.23) and (2.2.24) can now be invoked in Eq.(2.2.3) to obtain, with the help of Eq.(2.2.6), the following dressed equation for the evolution of the slow variable $s(t, \omega t)$, which now looks like

$$\ddot{s} + \gamma \dot{s} + (\tilde{\omega}^2 - \omega_0^2 q \cos \omega_p t) s + \alpha s^3 = c \cos \omega t \tag{2.2.25}$$

where the new frequency term $\tilde{\omega}$ is given by

$$\begin{aligned}\tilde{\omega}^2(g) &= \frac{3}{2}\alpha\langle f^2\rangle - \omega_0^2 \\ &= \frac{3}{4}\alpha g^2 \sum_{i=1}^{3} \frac{1}{\mu_i^2} - \omega_0^2. \end{aligned} \tag{2.2.26}$$

Among several parameters on which $\tilde{\omega}$ depends, in Eq.(2.2.26) specific emphasis has been laid on the dependence of $\tilde{\omega}$ on the strength (g) of the high-frequency forcing ($g\cos\Omega t$), because it is with the variation of g that the nonlinear response of the system will be studied. From the coefficient of s in Eq.(2.2.25) we conclude that the sought after time-dependent effective frequency can now be defined as

$$\omega_{eff}(t) = \sqrt{\tilde{\omega}^2 - \omega_0^2 q\cos\omega_p t}. \tag{2.2.27}$$

The coefficient of s for a Duffing oscillator should always remain positive thus giving rise, in this case, to a time-dependent effective potential representing an oscillating monostable quartic trap given as

$$V_{eff}(s,t) = \frac{1}{2}\omega_{eff}^2(t)s^2 + \frac{1}{4}s^4. \tag{2.2.28}$$

From a comparison between Eqs.(2.2.1) and (2.2.25) it becomes clear that a structural modification has been achieved. The coefficient of the x-term in

Eq.(2.2.1) is $[-\omega_0^2(1+q\cos\omega_p t)]$ which, by our requirement, is negative so as to give a symmetrically oscillating bistable potential. If in addition to this we further require that the coefficient of the s-term in Eq.(2.2.25) is positive, i.e., $(\tilde{\omega}^2 - \omega_0^2 q\cos\omega_p t) > 0$, then this effective equation describes a forced Duffing oscillator in an oscillatory monostable potential. This modification from a bistable to a monostable potential has been effected by the high-frequency forcing term $(g\cos\Omega t)$ sitting on the right hand side of Eq.(2.2.1). In the discussion following Eq.(2.2.2) we saw that for bistability we must have $-1 < q < 1$. For monostability of the modified potential we further require that $-\tilde{\omega}^2 < q\omega_0^2 < \tilde{\omega}^2$. These two conditions assure us that there exists a window in the parameter space where this interesting modification of a *parametrically oscillating bistable* potential to a *parametrically oscillating monostable* potential can be observed.

The flow equations

In the above calculations, the role of the low-frequency drive $(c\cos\omega t)$ has not come into focus. In this rather brief subsection, we shall derive the amplitude-flow and the phase-flow equations that follow from Eq.(2.2.25), to first order in perturbation theory. To this effect, we refer back to Eq.(2.2.2) and rewrite Eq.(2.2.25) as

$$\ddot{s} + \gamma\dot{s} + (\tilde{\omega}^2 - \omega_0^2 q\cos\omega t)s + \alpha s^3 = c\cos\omega t \tag{2.2.29}$$

thus recalling the main objective of the present chapter which, as mentioned in the discussion preceding Eq.(2.2.1), is to study the nonlinear response when the frequency of the parametric oscillation coincides with that of the low-frequency drive. To be more focussed, here our aim is to explore the response of the system close to what may be called the primary resonance, i.e., by tuning ω close to the frequency $\tilde{\omega}$ given by Eq.(2.2.26). To do this we introduce a detuning parameter $\tilde{\sigma}$ such that $\omega = \tilde{\omega} + \epsilon\tilde{\sigma}$, where ϵ is a perturbation parameter. The indispensability of perturbation theory in deriving amplitude and phase flow equations for nonlinear systems can hardly be overestimated and is a standard textbook material discussed in almost all books on nonlinear differential equations [65]. Therefore, without going into mathematical details, we mention the key points only. The perturbative approach starts with the initial rearrangement of Eq.(2.2.29) as

$$\ddot{s} + \tilde{\omega}^2 s = \epsilon[-\gamma\dot{s} + \omega_0^2 q(\cos\omega t)s - \alpha s^3 + c\cos\omega t] \tag{2.2.30}$$

where the perturbation parameter ϵ has been introduced for book-keeping purpose. This being an oscillatory system, the unperturbed (zeroth order) solution should be harmonic, over which the terms sitting on the right hand side of Eq.(2.2.30) exert their effects to modify it at the first order. Calculations become simpler on introducing a dimensionless time $\tau = \omega t$ and rewriting Eq.(2.2.30) as

$$s'' + s = \epsilon[-\Gamma s' + K(\cos\tau)s - \Lambda s^3 + C\cos\tau + \sigma s] \tag{2.2.31}$$

where primes denote derivatives with respect to τ and the new constants are defined as: $\Gamma = \gamma/\omega$, $K = \omega_0^2 q/\omega^2$, $\Lambda = \alpha/\omega^2$ and $C = c/\omega^2$. To first order in ϵ, the modified detuning parameter is $\sigma = 2\tilde{\sigma}\tilde{\omega}/\omega^2$ and is identified as

$$\frac{\tilde{\omega}^2}{\omega^2} = 1 - \epsilon\sigma. \tag{2.2.32}$$

Now, invoking the perturbative expansion $s(\tau_0, \tau_1) = s_0(\tau_0, \tau_1) + \epsilon s_1(\tau_0, \tau_1) + ...$ in Eq.(2.2.31) one obtains the unperturbed (zeroth order) solution $s_0 = a\cos(\tau + \theta)$ to the zeroth order equation $s_0'' + s_0 = 0$. The amplitude a and the phase θ are constants only at this order. As one proceeds to the first order, (a, θ) become time-dependent and equations for their first derivatives with respect to time are given as

$$
\begin{aligned}
s_1'' + s_1 &= -2\frac{\partial^2}{\partial\tau_0\partial\tau_1}s_0 - \Gamma s_0' + K(\cos\tau_0)s_0 \\
&- \Lambda s_0^3 + C\cos\tau_0 + \sigma s_0 \\
&= -2\frac{\partial^2}{\partial\tau_0\partial\tau_1}\big[a(\tau_1)\cos(\tau_0+\theta(\tau_1))\big] + \Gamma a\sin(\tau_0+\theta) \\
&+ K(\cos\tau_0)a\cos(\tau_0+\theta) - \Lambda a^3\cos^3(\tau_0+\theta) + \sigma a\cos(\tau_0+\theta) \\
&+ C\cos(\tau_0+\theta-\theta) \\
&= 2\big[\frac{\partial a}{\partial\tau_1}\sin(\tau_0+\theta) + a\cos(\tau_0+\theta)\frac{\partial\theta}{\partial\tau_1}\big] - \frac{3}{4}\Lambda a^3\cos(\tau_0+\theta) + \frac{Ka}{2}\cos(2\tau_0+\theta) \\
&+ \frac{Ka}{2}\cos(\theta) + \sigma a\cos(\tau_0+\theta) + \Gamma a\sin(\tau_0+\theta) + C\cos(\tau_0+\theta)\cos\theta \\
&+ C\sin(\tau_0+\theta)\sin\theta \qquad (2.2.33)
\end{aligned}
$$

after collecting the coefficients of $\sin(\tau_0+\theta)$ and $\cos(\tau_0+\theta)$ and separately equate them to zero give our sought after flow equations. They are obtained as

$$
\begin{aligned}
\frac{da}{d\tau} &= -\frac{1}{2}(\Gamma a + C\sin\theta) \qquad (2.2.34) \\
\frac{d\theta}{d\tau} &= \frac{1}{2}\left(\frac{3\Lambda}{4}a^2 - \sigma - \frac{C}{a}\cos\theta\right). \qquad (2.2.35)
\end{aligned}
$$

For the fixed point(s) (a_0, θ_0) of this dynamical system $\frac{da_0}{d\tau} = \frac{d\theta_0}{d\tau} = 0$ and we obtain the following quadratic equation in the modified detuning parameter σ as by squaring and adding (2.2.34) and (2.2.35)

$$\frac{C^2}{a_0^2} = \left(\frac{3\Lambda}{4}a_0^2 - \sigma\right)^2 + \Gamma^2$$
$$\implies \sigma^2 - \frac{3\Lambda a_0^2}{2}\sigma + \left(\Gamma^2 + \frac{9\Lambda^2}{16}a_0^4 - \frac{C^2}{a_0^2}\right) = 0.$$
$$\implies \sigma = \frac{3\alpha}{4}a_0^2 \pm \sqrt{\frac{c^2}{a_0^2} - \omega^2\gamma^2} \tag{2.2.36}$$

Now putting the solution of Eq.(2.2.36) in Eq.(2.2.32) we obtain

$$\tilde{\omega}^2 = \omega^2 - \epsilon\left[\frac{3\alpha}{4}a_0^2 \pm \sqrt{\frac{c^2}{a_0^2} - \omega^2 = \gamma^2}\right]$$
$$\frac{3M}{4}\alpha g^2 - \omega_0^2 = \omega^2 - \epsilon\left[\frac{3\alpha}{4}a_0^2 \pm \sqrt{\frac{c^2}{a_0^2} - \omega^2\gamma^2}\right] \tag{2.2.37}$$

where the old constants α, c and γ have been substituted back [see the lines between Eqs.(2.2.31) and (2.2.32)]. Finally we obtain the expression of g as

$$g(a_0) = \sqrt{\frac{1}{M}\left[\frac{4}{3\alpha}\left\{(\omega^2 + \omega_0^2) \pm \epsilon\sqrt{\frac{c^2}{a_0^2} - \omega^2\gamma^2}\right\} - \epsilon a_0^2\right]} \tag{2.2.38}$$

with M given as

$$M = \sum_{i=1}^{3}\frac{1}{\mu_i^2}. \tag{2.2.39}$$

In Eq.(2.2.38) we obtain a functional relation between the nonlinear response amplitude (a_0) and the strength of the high-frequency drive (g). In compliance with what was pointed out in the closing paragraph of Section-II, we see that the role of the high-frequency forcing is to enhance the resonant response to the low-frequency drive. It is also worth noting that in the flow equations [Eqs.(2.2.34) and (2.2.35)], the parameter q is absent thus signifying that the parametric oscillation does not dictate the flow at this order of perturbation. The parameter q enters the final relation [Eq.(2.2.38)] only through M. This point was also alluded to in the last paragraph of Section-II. In the following Section we plot the functional relation between a_0 and g for different values of Ω and observe reasonable agreement with numerical simulations.

2.3 Numerical simulations and discussions

The analytical result Eq.(2.2.38), that gives us a relation between the response amplitude a_0 and the control parameter g, has been plotted in Fig.(2.1) by dashed lines for different values of Ω, with the values of the relevant parameters chosen as $\omega_0 = 0.3$, $\gamma = 0.3$ and $\alpha = 0.05$. The dimensional amplitude pertaining to parametric excitation is set to the value $q = 0.5$. In the discussion following Eq.(2.1.1) the range of q was shown to be the same as that of $\cos\omega_p t$, viz. $-1 < q < 1$, and since they appear in product, it is sufficient to confine to the region $0 < q < 1$. Here our concern being the occurrence of the primary resonance, the amplitude and frequency of the

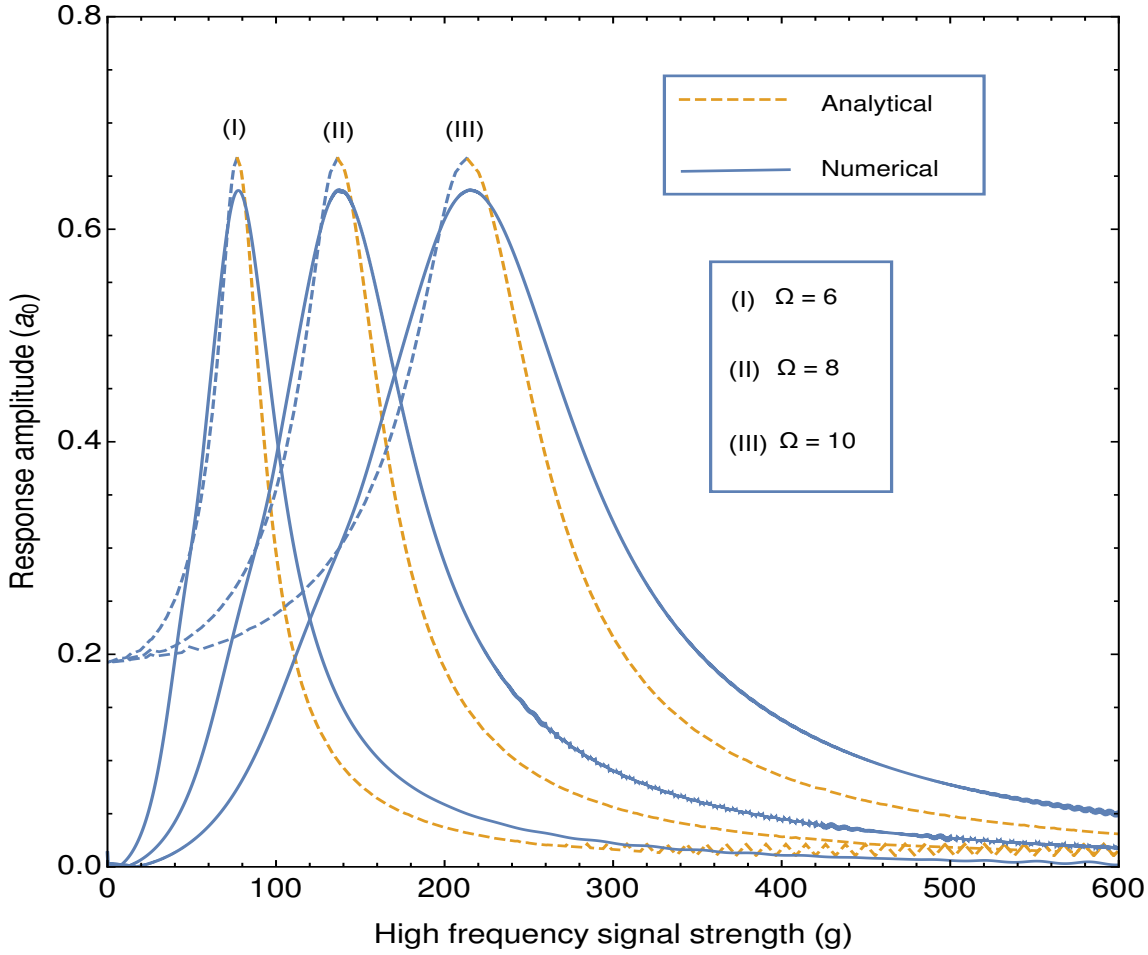

Figure 2.1: Response amplitude (a_0) as function of the strength (g) of the high-frequency excitation for a fixed set of parameters $\omega_0 = 0.3$, $q = 0.5$, $\gamma = 0.3$, $\alpha = 0.05$, $c = 0.06$ and $\omega_p = \omega = 0.3$, at different values of Ω. Analytical plots (dashed lines) are based on Eq.(2.2.38) and the numerical results (solid lines) are based on eqn.(2.1.1)

slow drive ($c\cos\omega t$) are taken to be $c = 0.04$ and $\omega = 0.3$ respectively. By observing the analytical result it transpires that in spite of a small periodic excitation of low frequency, we can get a pronounced resonance effect and

the response peak occurs at higher values of the control parameter g as we increase the value of Ω. It also appears that the resonance width expands with increasing values of Ω.

To validate our theoretical observations we perform numerical simulations on the starting model given in Eq.(2.1.1) and the results are shown by the solid lines in Fig.(2.1). The numerical method follows the one originally proposed in the revered work of Landa and McClintock [10]. In the presence of the nonlinearities the output signal $x(t)$ of Eq.(2.1.1) will be a mixture of several harmonics among which, our interest being to see the response of the system close to the primary resonance, we can write down the Fourier sine and cosine coefficients for the harmonic frequency ω as

$$B_s(\omega) = \frac{2}{nT}\int_0^{nT} x(t)\sin(\omega t)dt \tag{2.3.1}$$

$$B_c(\omega) = \frac{2}{nT}\int_0^{nT} x(t)\cos(\omega t)dt. \tag{2.3.2}$$

The $x(t)$ obtained by numerically solving the differential equation Eq.(2.1.1) is fed into the expressions for $B_s(\omega)$ and $B_c(\omega)$ to finally obtain the nonlinear amplitude defined as

$$a_0(\omega) = \frac{1}{c}\sqrt{B_s^2(\omega) + B_c^2(\omega)} \tag{2.3.3}$$

depicted by the solid lines in Fig.(2.1).

Though the numerical results comply satisfactorily with the analytical results, we cannot expect them to merge exactly. The plausible reason behind these unavoidable differences may be twofold. First, the analytical calculations have been done by separating the dynamics in only two time scales, one fast and the other slow, from where the fast variable has been averaged out to obtain the reduced effective system Eq.(2.2.29), from which the flow equations and thence the working formula Eq.(2.2.38) have been eventually derived and plotted. On the other hand, direct numerical integration of Eq.(2.1.1) preserves all the time scales of the dynamics automatically. Second, while deriving the flow equations, we have confined the calculations only to first order in perturbation theory, i.e., the dynamical variable s is taken to order $O(\epsilon)$ and the higher orders have been neglected.

Coming back to Fig.(2.1), it is also observed that for higher values of Ω, width of the numerical response curve is broader than that for the analytical one, while for lower values of Ω the agreement is better. In Fig.(2.2a) we find that the position of g_{max} (strength of the high frequency signal at response peak) is higher for higher values of Ω. Variation of g_{max} with respect to the external low signal strength c is shown in Fig.(2.2b) and here g_{max} is found to decrease as we increase the strength c.

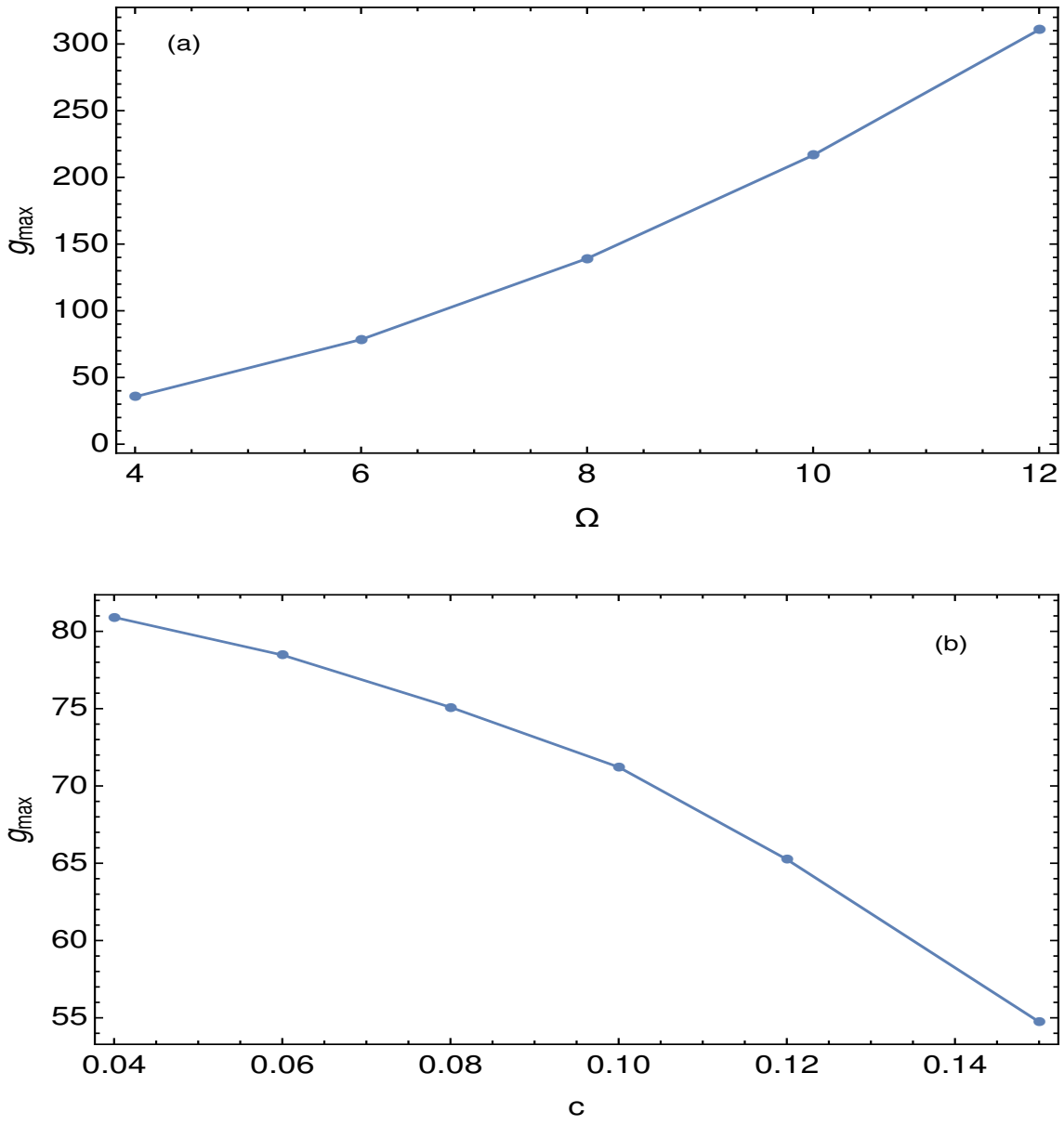

Figure 2.2: Numerical result for the position of maximum g_{max} of the non-linear response amplitude: (a) as a function of fast frequency (Ω) and for $c = 0.06$, $\gamma = 0.3$, $\alpha = 0.05$ and $\omega = \omega_p = 0.3$. (b)as a function of the slow frequency signal strength c for $\Omega = 6$, $\gamma = 0.3$, $\alpha = 0.05$ and $\omega = \omega_p = 0.3$

2.4 Summary

In summary, we have utilized the concept of vibrational resonance originally proposed by Landa and McClintock [10] to study the resonant response of a parametrically driven bistable oscillator. Apart from the parametric excitation, the oscillator is subjected to two other drives, one with a low frequency that is equal to the frequency of the parametric drive, and the other of a much higher frequency, the latter being the key player in the entire study. We have taken a flow equation approach by tuning the time-independent part of an effective frequency, that emerges on averaging out the effect of the high-frequency drive, perturbatively close to the frequency of the slow drive, the tuning being done by modulating only the strength of the high-frequency drive. The averaging procedure, just mentioned, transforms the original equation representing a symmetrically oscillating bistable potential to an effective equation representing a symmetrically oscillating monostable potential for a certain range of the values of the parameters involved, thus allowing us to take a perturbative approach on purely oscillatory base (unperturbed) solutions. The resonance condition obtained at the fixed point of a dynamical system described by the perturbatively obtained amplitude and phase flow equations is observed to conform reasonably with results obtained from numerical simulations. The response of the system has been studied, both analytically and numerically, as a function of the strength of the high-frequency drive which is used as the control parameter.

In the literature, responses of parametrically driven oscillators are usually studied on the basis of primary resonance defined about the natural frequency of the system, viz., some frequency analogous to ω_0 of Eq.(2.1.1) of this chapter. A subtle advantage of studying such resonant responses is that, ranges of different parameter values (for example, the damping constant(γ),parametric excitation strength(q)) required for sustained oscillations can be easily inferred on the basis of traditional harmonic balance methods. Furthermore, these methods can also be extended to include responses at subharmonic frequencies (defined as simple fractions of the natural frequency ω_0) as well, within the same ambit ([34]). In these regimes, of course, the systems under study offer rich plethora of phenomena to be studied. In the present work, however, we have defined the primary resonance, not about ω_0, but about some $\tilde{\omega}$ which is the time-independent part of an effective frequency that emerges as a result of averaging out the fast frequency contributions in the dynamics. As a result of this shift from the traditional definition of primary resonance, harmonic balance methods do not show up any critical value of the damping constant for sustenance of the oscillations. In fact, these studies are focussed on a different region of the frequency scale, and hence observations pertaining to nonlinear responses will also be different from those made close to the natural frequency of the system. Primarily, using the parameter q as a tool to convert an initially bistable system to an effective monostable one, so that all known phenomena connected to a forced Duffing oscillator can be studied for a bistable oscillator also, can be deemed as the main focus

of the present chapter.

In context of the aforementioned observations, in future it may be worthwhile to explore the other well known properties of the forced Duffing oscillator close to the primary resonance, for example, irreversible behaviour of the response amplitude as a function of the detuning parameter. Extension of such studies to subharmonic frequencies defined as natural fractions of the effective frequency is also expected to reveal interesting results. Two more aspects are also worthy of mention here. First, any perturbative study in any area of physics always leaves behind the issue of how close to the exact numerical results have the analytical predictions gone. Clearly, this chapter is not exempted from this question. The little disparity between the numerical and analytical predictions made at the first order of perturbation may only be expected to be ameliorated at the second order of perturbative calculations, although the accuracy depends on the perturbation method used. Comparative study of predictions at the second order made by well-known perturbative techniques, viz., the renormalization group, multiple-time scale analysis, generalized averaging procedures etc. to explore the fate of the analytical predictions at this order surely remains as an important future work to be pursued. Second, the possibility of transition of a forced Duffing oscillator to chaos, decided by certain properties of the Melnikov integral, is an exhaustively studied topic [65]. That this transition to chaos can be controlled by some parameter (for example, the strength of the rapid-frequency excitation) of the system, is also another potential area of study in future.

Chapter 3

Vibrational Resonance and Hopf Bifurcation in a Bistable van der Pol-Mathieu-Duffing Oscillator

- **Motivation of this Chapter**

  The response of specific nonlinear systems to a weak signal enhanced by the presence of fast harmonic signal drive has been the central motivation behind all studies concerning vibrational resonance(VR) for the last two decades. After originally proposed by McClintock and Landa

[10], a profusion of investigations have been carried out theoretically [11, 12], numerically [13] and experimentally [14, 15] with the special prominence given to nonlinear potentials [16, 17, 18, 19, 20, 21, 22, 23, 24, 25] in the backdrop of VR. Parametrically excited oscillators belong to such a family of nonlinear oscillators, which have been used extensively for the realization of various physical systems in science and engineering[38, 39, 40, 41, 42, 43]. The response of a parametric oscillator, whether stable or unstable under the action of biharmonic forces, requires special attention. Although extensive research has been pursued on the response of a high-frequency excited parametric oscillator [44, 45, 46, 48, 49, 50], studies of VR with slowly excited parametric oscillators have not, to the best of our knowledge, prominently come to focus [51, 34]. We further note that in addition to the time dependence of the natural frequency of a parametric oscillator, if the system operates in a spatially nonlinear dissipative medium, then the response of the system to an additive combination of external low and high-frequency drives is an interesting problem in its own right.

In this chapter, we consider van der Pol-Mathieu-Duffing(VMD) oscillator, a typical parametric oscillator with nonlinear damping and two externally acting forcing terms with two widely different frequencies. The intrinsic property of self-excitation of a van der Pol oscillator combines with the parametric excitation allow us to study a more general class of parametric oscillators. Applications of this model can be found

directly in various MEMS devices [53, 54].A thorough investigation of non-trivial effects of the high-frequency drive affecting the stability of the slow dynamics through modification of some governing parameters have been considered in recent times [56, 57, 58, 60]. However, the nonlinear response of VMD under multiple external forcing with different orders of strength and frequency has remained less explored and is one of our motivations In this chapter. In Sec. (**3.1**), the framework of the model and the justifications are described. In Sec. (**3.2**), (**3.3**) and (**3.4**) the detailed mathematical techniques followed by numerical simulations are given. Finally, this chapter is concluded in Sec. (**3.5**).

3.1 One dimensional Van der Pol-Mathieu-Duffing oscillator

The typical mathematical model of a VMD oscillator consists of a nonlinear damping term, an oscillatory stiffness and a nonlinear stiffness controlled by two external forcing drives with widely different frequencies. The rationale behind such an arrangement of terms in the context of VR has been discussed in the Introduction. The dynamical equation is given by

$$\ddot{x} + \gamma(x^2 - 1)\dot{x} + \omega_0^2(1 + h\cos\omega_p t)x + \alpha x^3 = c\cos\omega t + g\cos\Omega t \qquad (3.1.1)$$

where $h\cos\omega_p t$ is the parametric excitation with strength h and $c\cos\omega t$ and $g\cos\Omega t$ are the slow and fast frequency drive respectively with $\Omega \gg \omega$. As we consider the parametric excitation to be small, without loss of generality we can set $\omega_p = 2\omega$ and the reason behind this particular chosen value is clarified in the following paragraph. Now depending on the sign of ω_0^2 and α, three potential structures may arise viz. (a) single well ($\omega_0^2 > 0$, $\alpha > 0$) (b) double well ($\omega_0^2 < 0$, $\alpha > 0$) and (c) double hump ($\omega_0^2 > 0$, $\alpha < 0$). Our model here describes the dynamics of a VDM oscillator under a time dependent double well potential,

$$\ddot{x} + \gamma(x^2 - 1)\dot{x} - \omega_0^2(1 + h\cos\omega_p t)x + \alpha x^3 = c\cos\omega t + g\cos\Omega t \qquad (3.1.2)$$

Therefore the oscillator is on the crest of a double well and is in an unstable equilibrium provided the excitation strength h is confined to the domain $-1 < h < 1$. The effect of the high-frequency drive ($g\cos\omega t$) is to redress the double well potential into a single well,thus effectively changing the stability concerning the slow-motion of the oscillator [51, 23]. In this chapter, we shall show that this high-forcing drive changes the potential structure through

an effective modification of the natural stiffness and reshapes the damping function reflected in the slow dynamics of the original system (3.1.1). Our theoretical study regarding the combined role of the excitation forcing h and the excitation frequencies ω_p and Ω in delicately amending the oscillation frequency and the damping term satisfactorily complies with the numerical results. In order to notice the resonant response to the slow drive $c\cos\omega t$, the contribution of h is only perceptible for non zero fast forcing strength, i.e. $g \neq 0$ and show up in the flow equations which has been elucidated in the next section. Before proceeding to the next section, it is noteworthy that ω_p and ω are entirely two different frequencies and have a subtle role in modifying the system parameters. However, in our chapter, we consider $\omega_p = 2\omega$, keeping in mind that our sole motivation is to study the system's response close to the unperturbed or the natural frequency(ω_0) of the system [34]. In our analytical description for deriving the response curve that finally leads to the formation of a limit cycle, we have used multiple time-scale analysis to the first order in perturbation. The choice of the excitation frequency as being twice the external forcing frequency allows the effect of the parametric excitation (h) to be felt in the flow equations at the very first order in perturbation [66].

3.2 The effective slow dynamics

To analyze the effect of fast forcing drive to the system (3.1.1), we use the method of direct partition of motion [12]. To implement this method in the

system one considers two time scales, one slow and the other fast, so that the dynamical variable can be written as a sum of a slow variable $s \equiv s(t, \omega t)$ and a fast variable $f \equiv f(t, \Omega t)$, viz.,

$$x(t) = s(t, \omega t) + f(t, \Omega t). \tag{3.2.1}$$

Here f is a periodic function and has a zero mean over a complete period as

$$\langle f \rangle = \frac{1}{2\pi} \int_0^{2\pi} f \; d\tau = 0 \tag{3.2.2}$$

where $\tau = \Omega t$ is the dimensionless time corresponding to the fast time scale. Substituting equations Eqs.(3.2.1) and (3.2.2) into Eq. (3.1.1) we can write the dynamical equation for the slow variable as

$$\ddot{s} + \gamma(s^2 + 2s\langle f \rangle + \langle f^2 \rangle - 1)\dot{s} - F_0(t)s + \alpha F_1(s, f) = c\cos\omega t \tag{3.2.3}$$

and for the fast variable as

$$\begin{aligned} \ddot{f} + \gamma(s^2 + \quad & 2s \quad [f - \langle f \rangle] + [f^2 - \langle f^2 \rangle] - 1)\dot{f} - F_0(t)f \\ + \quad & \alpha F_2(s, f) = g\cos\Omega t \end{aligned} \tag{3.2.4}$$

where the term containing the parametric excitation is given by

$$F_0(t) = \omega_0^2(1 + h\cos\omega_p t). \tag{3.2.5}$$

The two functions associated with the parameter α in eqs.(3.2.3) and (3.2.4) are given by

$$F_1(s,f) = s^3 + 3s^2\langle f\rangle + 3s\langle f^2\rangle + \langle f^3\rangle \tag{3.2.6}$$

$$\begin{aligned} F_2(s,f) &= 3s^2(f - \langle f\rangle) + 3s(f^2 - \langle f^2\rangle) \\ &+ (f^3 - \langle f^3\rangle). \end{aligned} \tag{3.2.7}$$

Now f being a fast variable, one can assume that $\ddot{f}, \dot{f} \gg f, f^2, f^3$ etc, and by invoking this assumption in Eq.(3.2.4) and then solving it in a self-consistent way [24], by taking only the linear terms, we can arrive at the equation

$$\ddot{f} - \gamma\dot{f} = gB \cos(\Omega t + \eta) \tag{3.2.8}$$

The amplitude factor of Eq. (3.2.8) has the form

$$B = \sqrt{(1 + A\cos\beta)^2 + (A\sin\beta)^2} \tag{3.2.9}$$

where the dimensionless amplitude factor reads

$$A = \frac{\omega_0^2}{\Omega\sqrt{\Omega^2 + \gamma^2}}, \tag{3.2.10}$$

along with this, the newly introduced phase factors

$$\beta = -\tan^{-1}\left(\frac{\gamma}{\Omega}\right) \tag{3.2.11}$$

$$\eta = \tan^{-1}\left(\frac{A\sin\beta}{1 + A\cos\beta}\right). \tag{3.2.12}$$

Eq. (3.2.8) yields the solution

$$f(t) = \frac{g}{\kappa}\cos(\Omega t + \eta + \theta). \tag{3.2.13}$$

the associated phase term

$$\theta = -\tan^{-1}\left(\frac{\gamma}{\Omega}\right) \tag{3.2.14}$$

and the constant κ appearing in the amplitude factor of Eq. (3.2.13) reads

$$\kappa = \frac{\Omega^2(\Omega^2+\gamma^2)}{\sqrt{(\Omega^2-\omega_0^2)^2+\Omega^2\gamma^2}} \tag{3.2.15}$$

It can be seen that these constants are proportional to Ω^2 for large values of Ω, so that the contribution of the fast variable $f(t)$ to the main governing dynamics of the system (given by Eq. (3.1.1)) becomes small, thus justifying the efficacy of this method of solving the differential equation self consistently. Further, the harmonic nature of the solution for $f(t)$ yields the averages

$$\langle f\rangle = \langle f^3\rangle = 0 \tag{3.2.16}$$

$$\langle f^2\rangle = \frac{g^2}{2}M \tag{3.2.17}$$

where

$$M = \frac{1}{\kappa^2}. \tag{3.2.18}$$

Using these above averages along with Eqs.(3.2.6) and (3.2.7) in the equation of motion given by Eq. (3.2.3), we get an effective equation for the slow variable as

$$\ddot{s} + \gamma(s^2 + K)\dot{s} + (\tilde{\omega}^2 - \omega_0^2 h \cos\omega_p t)s + \alpha s^3 = c\cos\omega t \tag{3.2.19}$$

where the frequency term $\tilde{\omega}$ is given by

$$\begin{aligned} \tilde{\omega}^2(g) &= 3\alpha\left\langle f^2\right\rangle - \omega_0^2 \\ &= \frac{3}{2}\alpha g^2 M - \omega_0^2 \end{aligned} \tag{3.2.20}$$

and the factor associated with the nonlinear damping K takes the form

$$K(g) = \frac{g^2}{2}M - 1. \tag{3.2.21}$$

It is now evident that Eq. (3.2.19) represents a monostable van der Pol-Duffing oscillator under the influence of the potential

$$V_{mono}(s,t) = \frac{1}{2}\omega_{eff}^2(t)s^2 + \frac{1}{4}\alpha s^4 \tag{3.2.22}$$

where the centrally important effective frequency has the form

$$\omega_{eff} = \sqrt{(\tilde{\omega}^2 - \omega_0^2 h \cos \omega_p t)}. \tag{3.2.23}$$

A close observation of Eq. (3.2.19) reveals that a structural modification has been achieved for a specific range of certain parameters. The coefficient of x in Eq. (3.1.1) will be negative if we set the parametric excitation strength h to lie within the range $-1 < h < 1$, thus making the oscillator of Eq. (3.1.1) bistable. This bistability gets modified to an effective monostability if, in addition to the above condition on h, we also set $-\tilde{\omega}^2 < \omega_0^2 h < \tilde{\omega}^2$. This is the central role played by the fast forcing term $g \cos \Omega t$,which in effect changes the natural frequency ω_0 to the new value $\tilde{\omega}$.

3.3 Slow flow and the the resonance response

We rewrite Eq. (3.2.19) by setting the parametric excitation frequency $\omega_p = 2\omega$

$$\ddot{s} + \gamma(s^2 + K)\dot{s} + (\tilde{\omega}^2 - \omega_0^2 h \cos 2\omega t)s + \alpha s^3 = c \cos \omega t \tag{3.3.1}$$

Our main objective in this study is to find out the response of the VMD oscillator to the external slow drive as we vary the strength of the rapidly oscillating field. To this end, we specifically focus our attention on the pri-

mary resonance, i.e., the response of the system whenever the frequency of the slow drive (ω) is tuned *perturbatively* close to the natural frequency of the slow motion ($\tilde{\omega}$). Rearranging Eq. (3.3.1) by the use of a dimensionless time $\tau = \omega t$ and defining $\omega = \tilde{\omega} + \epsilon\tilde{\sigma}$

$$s'' + s = \epsilon[-\Gamma(s^2 + K)s' + H(\cos 2\tau)s - \Lambda s^3 + C\cos\tau + \sigma s] \tag{3.3.2}$$

where we have introduced the detuning parameter σ and the primes denote derivatives with respect to τ. The perturbation parameter ϵ is introduced here to elucidate that all the terms excepting the two on the left-hand side of Eq. (3.3.2) are small. To this effect, we define the newly introduced parameters on the right hand side of (3.3.2) as: $\Gamma = \frac{\gamma}{\omega}$, $\Lambda = \frac{\alpha}{\omega^2}$, $C = \frac{c}{\omega^2}$ and $H = \frac{\omega_0^2 h}{\omega^2}$. Also, the σ appearing at the end of the above equation is defined as $\sigma = \frac{2\tilde{\sigma}\tilde{\omega}}{\omega^2}$ and is related to the ratio of the frequencies to first order in ϵ by

$$\frac{\tilde{\omega}^2}{\omega^2} = 1 - \epsilon\sigma \tag{3.3.3}$$

To derive the amplitude and phase flow equations we apply the multiple time scale analysis [66] to Eq. (3.3.2) by using perturbative expansion to first order in ϵ,

$$s(\tau_0, \tau_1) = s_0(\tau_0, \tau_1) + \epsilon s_1(\tau_0, \tau_1) + \mathcal{O}(\epsilon^2) \tag{3.3.4}$$

Here $\tau_i = \epsilon^i \tau$, so that $\tau_0 = \tau$ and $\tau_1 = \epsilon\tau$. The derivatives in terms of τ_i accordingly evaluates to $\frac{d}{d\tau} = \frac{\partial}{\partial\tau_0} + \epsilon\frac{\partial}{\partial\tau_1} + \mathcal{O}(\epsilon^2)$ and $\frac{d^2}{d\tau^2} = \frac{\partial^2}{\partial\tau_0^2} + 2\epsilon\frac{\partial^2}{\partial\tau_1\partial\tau_0} + \mathcal{O}(\epsilon^2)$. Substituting Eq. (3.3.4) into Eq. (3.3.2) and equating the coefficient of ϵ order by order we get

$$(\epsilon^0): \qquad s_0'' + s_0 = 0, \tag{3.3.5}$$

$$\begin{aligned}(\epsilon^1): \qquad s_1'' + s_1 &= -2\frac{\partial^2 s_0}{\partial\tau_1\partial\tau_0} - \Gamma(s_0^2 + K)s_0' \\ &+ H\cos(2\tau_0)s_0 - \Lambda s_0^3 \\ &+ C\cos\tau_0 + \sigma s_0.\end{aligned} \tag{3.3.6}$$

Solving the zeroth-order equation gives

$$s_0(\tau_0, \tau_1) = a(\tau_1)\cos(\tau_0 + \theta(\tau_1)). \tag{3.3.7}$$

Substituting Eq. (3.3.7) into Eq. (3.3.6) and equating the coefficient of

secular terms to zero gives the slow flow amplitude and phase equations as follows:

$$\frac{da}{d\tau} = -\frac{1}{2}\left[\frac{\Gamma a^3}{4} + \Gamma K a + C\sin\theta + \frac{Ha}{2}\sin(2\theta)\right] \tag{3.3.8}$$

$$\frac{d\theta}{d\tau} = \frac{1}{2}\left[\frac{3\Lambda}{4}a^2 - \sigma - \frac{C}{a}\cos\theta - \frac{H}{2}\cos(2\theta)\right] \tag{3.3.9}$$

The fixed point(s) are obtained by solving the equations (a_0, θ_0) give $\frac{da}{d\tau} = \frac{d\theta}{d\tau} = 0$ which, on combining, give the quadratic equation in σ

$$\begin{aligned}(\frac{3\Lambda}{4}a_0^2 - \sigma)^2 + (\frac{\Gamma a_0^2}{4} + \Gamma K)^2 &= \frac{C^2}{a_0^2} + \frac{H^2}{4} \\ &+ \frac{CH}{a_0}\cos\theta_0.\end{aligned} \tag{3.3.10}$$

Solving for the detuning parameter we get,

$$\sigma = \frac{3\Lambda}{4}a_0^2 + \sqrt{\frac{C^2}{a_0^2} + \frac{H^2}{4} + \frac{CH}{a_0}Y} \tag{3.3.11}$$

where the constant Y is the root of a quadratic equation in $\cos\theta_0$ obtained by putting the left-hand side of (3.3.9) to zero. Thus,

$$Y = \cos\theta_0 = \frac{-\frac{C}{a_0} \pm \sqrt{\frac{C^2}{a_0^2} + 4H\left(\frac{H}{2} + \frac{3\Lambda}{4}a_0^2 - \sigma\right)}}{2H} \tag{3.3.12}$$

Finally putting back the solution for σ in Eq. (3.3.11) into Eq. (3.3.3) and combining that with Eq. (3.2.20) we get the desired analytical expression for the fast excitation strength g as a function of amplitude a_0,

$$g(a_0) = \sqrt{\frac{1}{M}\left[\frac{2}{3\alpha}\left\{(\omega^2 + \omega_0^2) \pm \epsilon N\right\} - \frac{\epsilon a_0^2}{2}\right]} \tag{3.3.13}$$

$$\text{where} \qquad N = \sqrt{\frac{c^2}{a_0^2} + \frac{\omega_0^4 h}{4} + \frac{c^2\omega_0^2 h}{a_0}Y}$$

This is our sought after response for vibrational resonance. Conventionally, vibrational response is observed by calibrating the high frequency drive strength g. M.Zhan *et al* have showed that a simple bistable syatem can have a enhanced vibrational frequency resonance if one suitably controls the fast signal frequency Ω for a fixed value of g [59]. Following Eq. (3.3.14) it can

be concluded that,our proposed VMD system can also achieve this kind of frequency resonance response for suitably chosen values of parameters. The functional relation between the response amplitude and fast frequency Ω can be visualized as Fig.(3.2),

$$a_0(\Omega) = \sqrt{\frac{1}{\epsilon}\left[\frac{4}{3\alpha}\left\{(\omega^2 + \omega_0^2) \pm \epsilon N\right\} - 2g^2 M\right]} \tag{3.3.14}$$

To establish our analytical results we run numerical simulation on Eq. (3.1.1) as proposed in [10].The main idea is to extract the Fourier sine and cosine components of the harmonic frequency ω from the mixture of several harmonics present in the nonlinear output signal [x(t)]. We can express the sine and cosine components as

$$Q_s(\omega) = \frac{2}{mT}\int_0^{mT} x(t)\sin(\omega t)dt \tag{3.3.15}$$

$$Q_c(\omega) = \frac{2}{mT}\int_0^{mT} x(t)\cos(\omega t)dt \tag{3.3.16}$$

Now, using the RK-4 method to solve $x(t)$ from Eq. (3.1.1) and then putting back the values into the above equations and evaluating the integrals numerically, we finally get the nonlinear response amplitude

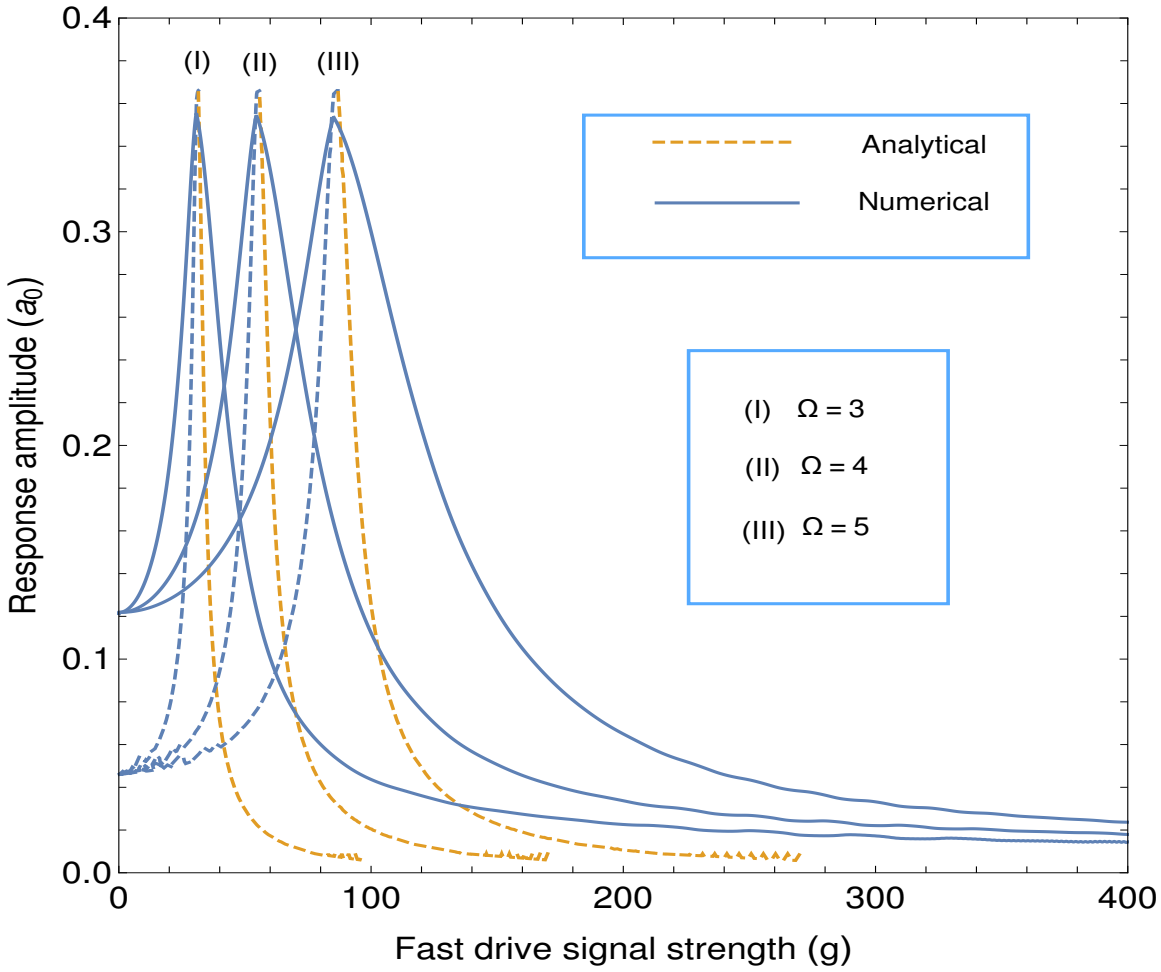

Figure 3.1: Response amplitude (a_0) as function of the strength (g) of the high-frequency excitation for a fixed set of parameters $\omega_0 = 0.3$, $h = 0.01$, $\gamma = 0.15$, $\alpha = 0.01$, $c = 0.05$ and $\omega_p = 0.6$ $\omega = 0.3$, at different values of Ω. Analytical plots (dashed lines) are based on Eq. (3.3.14) and the numerical results (solid lines) are based on Eq.(3.1.2)

$$a_0(\omega) = \frac{\sqrt{Q_s^2(\omega) + Q_c^2(\omega)}}{c} \tag{3.3.17}$$

which is shown in (Fig.3.1). Though our analytical expression Eq. (3.3.14) agrees reasonably with the numerical results. However, disagreement gradually creeps in for higher values of Ω; the possible reasons can be twofold. First, the original dynamics of the system is divided into two time scale, a fast and a slow one, from where the rapidly varying variable is averaged out to get an effective slow dynamics of the original system. The numerical integration, on the other hand, preserves all the time scales. Second, to derive the flow equations (Eqs.3.3.9 and 3.3.9) we restrict our calculations to order $\mathcal{O}(\epsilon)$ as opposed to the numerical approach that is ideally capable of reproducing almost exact results. This point, however, is generically applicable for all perturbative approaches.

Finally (Fig.3.3) states the variation of g_{max}(i.e. the value of fast drive strength g at response peak) with Ω and c.

3.4 Change in stability through Hopf bifurcation

The flow equations (Eqs.(3.3.9) and (3.3.9)) obtained for the slow variable by averaging out the fast variable from Eq. (3.1.1) can be further studied with the purpose of exploring the behaviour of limit cycle which is characteristic of a van der Pol oscillator. To understand the behaviour of the flow equations,

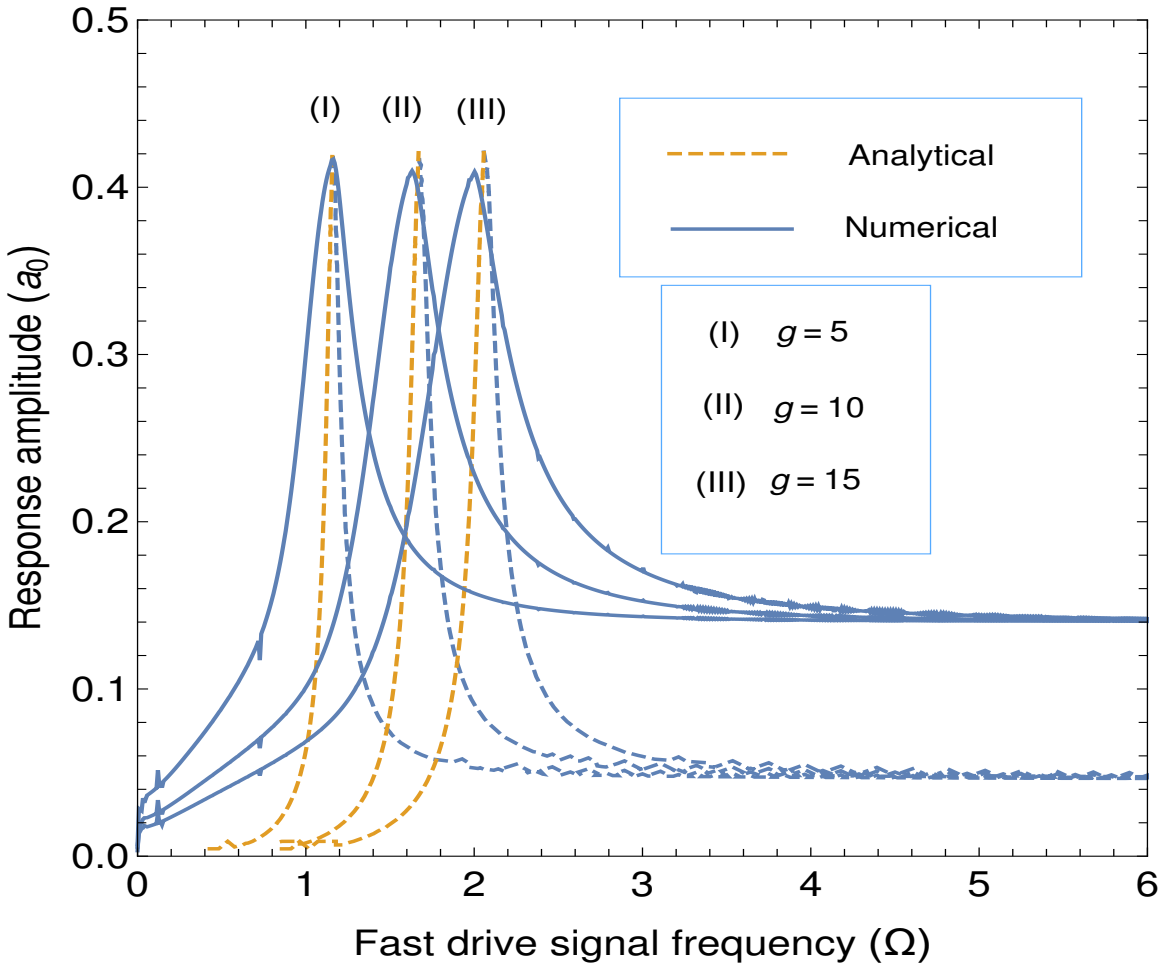

Figure 3.2: Response amplitude (a_0) as function of frequency Ω of the high-frequency excitation for a fixed set of parameters $\omega_0 = 0.3$, $h = 0.01$, $\gamma = 0.15$, $\alpha = 0.01$, $c = 0.05$ and $\omega_p = 0.6$ $\omega = 0.3$, at different values of g. Analytical plots (dashed lines) are based on Eq. (3.3.14) and the numerical results (solid lines) are based on Eq.(3.1.1)

we have to resort to perturbation theory yet again by introducing a new perturbation parameter λ. The limit cycle that transpires from the subsequent analysis represents an oscillation of the slow variable over a much longer time

scale, viz., $t \sim \mathcal{O}(1/\lambda\epsilon)$. In the literature, the new set of flow equations thus obtained by effecting a perturbative expansion for a second time goes by the name "super-slow flow" equations [67]. These equations eventually allow us to predict, with significant accuracy, the value of the control parameter g at which the effective slow dynamics goes through a *Hopf bifurcation* thus leading to the birth of a stable limit cycle.

3.4.1 The super-slow flow equations

To derive the super-slow flow equations, we parametrize the slow flow equations (Eqs.(3.3.9) and (3.3.9)) as

$$u = a\cos\theta \qquad \text{and} \qquad v = -a\sin\theta \tag{3.4.1.1}$$

so that,

$$\begin{aligned} \frac{du}{d\tau} &= (-\frac{\sigma}{2} + \frac{H}{4})v + \lambda\Big\{\frac{1}{8}(3\Lambda v - \Gamma u)(u^2+v^2) \\ &- \frac{\Gamma K u}{2}\Big\} \end{aligned} \tag{3.4.1.2}$$

$$\begin{aligned}\frac{dv}{d\tau} &= (\frac{\sigma}{2}+\frac{H}{4})u+\lambda\Big\{\frac{c}{2}-\frac{1}{8}(3\Lambda u+\Gamma v)(u^2+v^2)\\ &- \frac{\Gamma K v}{2}\Big\}\end{aligned} \tag{3.4.1.3}$$

where the newly brought in perturbation parameter λ has been invoked in such a way that the zeroth-order terms yield simple harmonic solutions for the variables u and v. This arrangement requires that we cluster the (modified) damping constant (Γ), nonlinearity (Λ) and the strength of the slow drive (c) under the common banner of the new perturbation parameter λ. In the spirit of multiple time scale analysis, we now invoke the perturbation expansions [47, 55] in λ as,

$$\begin{aligned}u(T_0,T_1) &= u_0(T_0,T_1)+\lambda u_1(T_0,T_1)+\mathcal{O}(\lambda^2)\\ v(T_0,T_1) &= v_0(T_0,T_1)+\lambda v_1(T_0,T_1)+\mathcal{O}(\lambda^2)\end{aligned} \tag{3.4.1.4}$$

where $T_j=\lambda^j\tau$. Now the derivatives in terms of variables T_i are connected to τ as $\frac{d}{d\tau}=D_0+\lambda D_1+\mathcal{O}(\lambda^2)$ where $D_j=\frac{\partial}{\partial T_j}$. Substituting the set of equations Eq. (3.4.1.4) into Eqs.(3.4.1.2) and (3.4.1.3) followed by separation of the terms in accordance with the powers of λ we get, the zeroth-order and the first order equations as follows:

$$(\lambda^0): \qquad D_0^2 u_0 + \omega_l^2 u_0 = 0 \tag{3.4.1.5}$$

$$-(\frac{\sigma}{2} - \frac{H}{4})v_0 = D_0 u_0 \tag{3.4.1.6}$$

$$\begin{aligned}(\lambda^1): \qquad D_0^2 u_1 + \omega_l^2 u_1 = &-(\frac{\sigma}{2} - \frac{H}{4})\Big[- D_1 v_0 + \frac{c}{2} \\ &- \frac{\Gamma K v_0}{2} - \frac{1}{8}(3\Lambda u_0 + \Gamma v_0)(u_0^2 + v_0^2)\Big] \\ &- D_0 D_1 u_0 - \frac{\Gamma K}{2} D_0 u_0 \\ &+ D_0\Big[\frac{1}{8}(3\Lambda v_0 - \Gamma u_0)(u_0^2 + v_0^2)\Big]\end{aligned} \tag{3.4.1.7}$$

$$\begin{aligned}-(\frac{\sigma}{2} - \frac{H}{4})v_1 = &\ D_0 u_1 + D_1 u_0 + \frac{\Gamma K u_0}{2} \\ &- \frac{1}{8}(3\Lambda v_0 - \Gamma u_0)(u_0^2 + v_0^2)\end{aligned} \tag{3.4.1.8}$$

where the super-slow oscillation frequency is defined as $\omega_l = \sqrt{\frac{\sigma^2}{4} - \frac{H^2}{16}}$. From Eqs.(3.4.1.5) and (3.4.1.6) we obtain the zeroth-order solution as

$$u_0 = r(T_1)\cos(\omega_l T_0 + \psi(T_1)) \tag{3.4.1.9}$$

$$v_0 = \frac{\omega_l}{p} r(T_1)\sin(\omega_l T_0 + \psi(T_1)) \tag{3.4.1.10}$$

where we define $p = (\frac{\sigma}{2} - \frac{H}{4})$. Now invoking Eqs.(3.4.1.9) and (3.4.1.10) into Eq. (3.4.1.7) and equating the secular terms to zero generates new set of flow equations as

$$D_1 r = \frac{-\Gamma K}{2} r - \frac{\sigma\Gamma}{8\sigma - 4H} r^3 \tag{3.4.1.11}$$

$$D_1 \psi = -\frac{9\Lambda\sigma^2}{4(2\sigma - H)\sqrt{(4\sigma^2 - H^2)}} r^2. \tag{3.4.1.12}$$

The equilibrium solution $D_1 r = 0$ gives the analytical estimate of the radius of the limit cycle

$$r = 0 \quad \text{and} \quad r = \sqrt{K(\frac{2H}{\sigma} - 4)} \tag{3.4.1.13}$$

where, through a linear stability analysis, we see that the origin is unstable while the second root of r, denoting the limit cycle, is stable. Clearly, this non-trivial root of r reveals the dependence of the amplitude of the limit

cycle on the fast drive strength g and the frequency Ω through $K(g)$ defined in Eq. (3.2.21). This analytical expression complies reasonably with the results obtained by numerically solving the system given by Eqs.(3.4.1.2) and (3.4.1.3) for different sets of (Ω), as has been shown in (Fig.3.4).

From Eq. (3.4.1.11), it is also clear that in the parametric space, $K = 0$ represents a point where a supercritical Hopf bifurcation occurs. When $K > 0$, the origin acts as the only stable fixed point. Looking back at Eq. (3.2.21) we see that by changing the control parameter g, we can change K. Therefore, when K becomes negative, we see that the origin is destabilized, and a stable limit cycle is created. This transition occurs at the point $K = 0$ which, according to Eq. (3.2.21), happens at the threshold value of g given by

$$g_{_{hopf}} = \sqrt{\frac{2}{M}}. \tag{3.4.1.14}$$

With the values of the parameters chosen as $\gamma = 0.15$, $\alpha = 0.1$, $c = 0.0005$, $\omega = \omega_0 = 0.3$ and $h = 0.01$, combining Eq.(3.2.15) and Eq. (3.2.18) we get $M = 0.012$ for $\Omega = 3$ and $M = 0.0038$ for $\Omega = 4$. Placing them one by one into Eq.(3.4.1.14) gives $g_{_{hopf}} = 12.88$ and $g_{_{hopf}} = 22.95$ respectively for $\Omega = 3$ and $\Omega = 4$. These values are in very good agreement with the data obtained

by numerically solving the equation of motion of the slow variable given by Eq. (3.3.1), as have been shown in Fig.(3.5) and Fig.(3.6).

3.5 Summary

To summarize, we have studied the parametric resonance of a van der Pol-Duffing oscillator under the influence of two periodic drives with widely different frequencies and have shown that the response of the system to the slow drive can be controlled by modulating the strength of the fast drive, g. Studies pertaining to *vibrational resonance* are usually modeled in this way. Although in literature there have been some contributions concerning the study of this parametric VMD oscillator driven by high- frequency excitation[44, 45, 46], the study and interpretation of nonlinear response in the backdrop of *vibrational resonance* on this type of system have, to the best of our knowledge, not been prominently pursued. The procedure of sieving out an effective slow dynamics by averaging out the fast variable has two important consequences. First, the symmetrically oscillating bistable potential (with the natural frequency ω_0) figuring in the starting differential equation Eq.(3.1.2) gets reshaped to a symmetrically oscillating monostable potential with a new frequency $\tilde{\omega}$ within a certain range of values of the parameters involved. In the majority of works regarding parametric resonance, dynamics close to the natural frequency (ω_0) or the parametric frequency (ω_p) have been studied, and the primary resonance is usually defined accord-

ingly. In this work, however, we have studied the dynamics by deriving flow equations for amplitude and phase, by effecting perturbation theory in the vicinity of the new frequency ($\tilde{\omega}$), and not around ω_0 or ω_p, thus leading to consequences not explored in earlier works. Second, the strength of the fast drive, g, also reshapes the damping by contributing an additional nonlinearity in the damping term of the initial dynamics described by Eq. (3.1.2). This modification has a pronounced effect on the formation of the limit cycle in the self-excited oscillator in that, by modulating g, one can control the position of the point in parameter-space where the all-important Hopf bifurcation should occur. In this context, we have been able to define a threshold value g named g_{hopf} below which the limit cycle should exist. By keeping g in this range, viz. $g < g_{hopf}$, one can adjust the fast frequency Ω as well as the strength of the parametric oscillation h so that there is a stable limit cycle oscillation in an effective monostable potential with a frequency given by ω_l evaluated in Sec.V.

The present study may have important applications in nano-mechanical oscillatory systems [61, 62]. Extensions of this study to understand the subharmonic and superharmonic responses for parametrically driven oscillators in the backdrop of vibrational resonance can have many interesting implications.

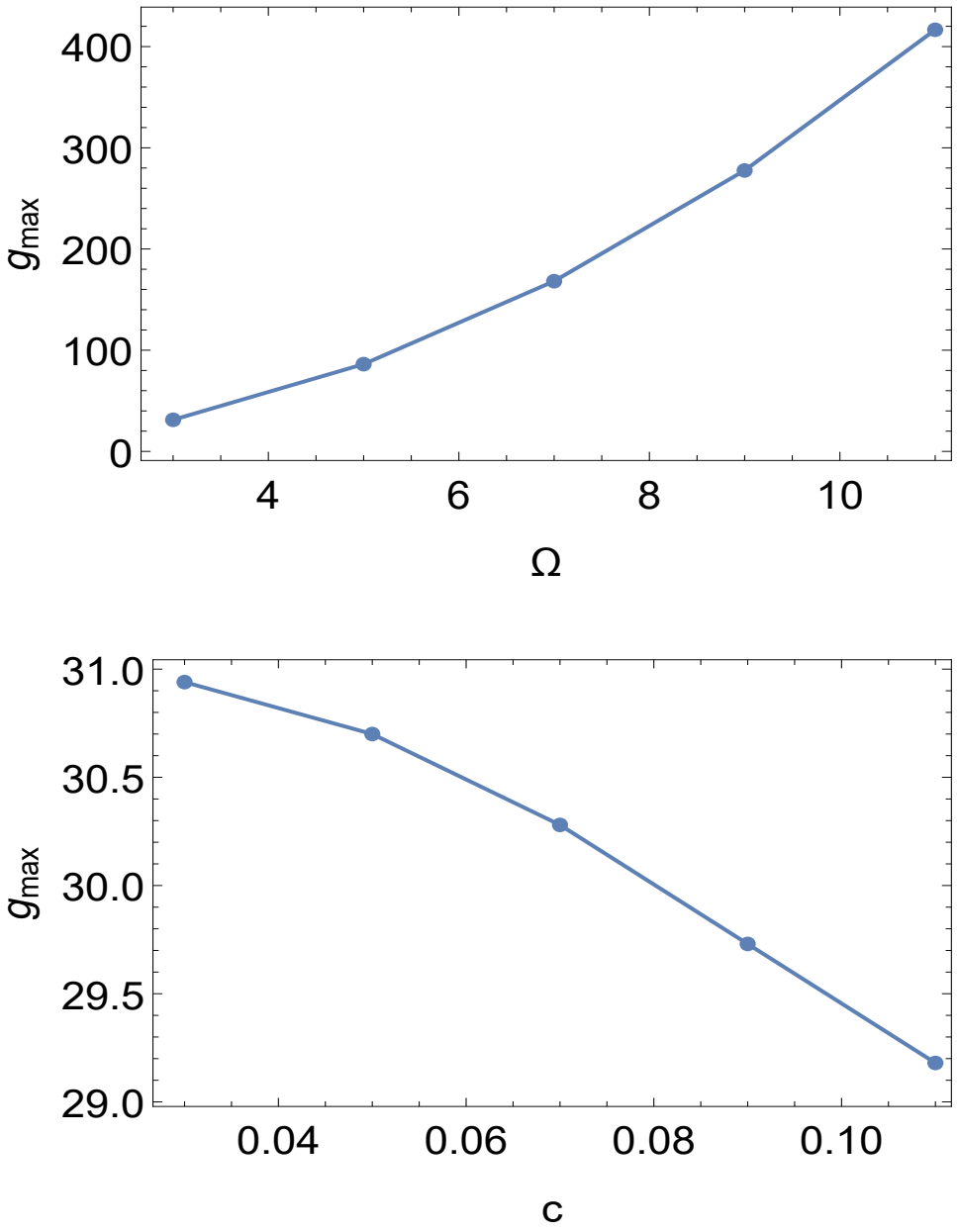

Figure 3.3: Numerical result for the position of maximum g_{max} of the non-linear response amplitude: (a) as a function of fast frequency (Ω) and for $c = 0.05$, $\gamma = 0.15$, $\alpha = 0.01$ and $\omega = \omega_p = 0.3$. (b)as a function of the slow-frequency signal strength c for $\Omega = 3$, $\gamma = 0.15$, $\alpha = 0.01$ and $\omega = \omega_p = 0.3$

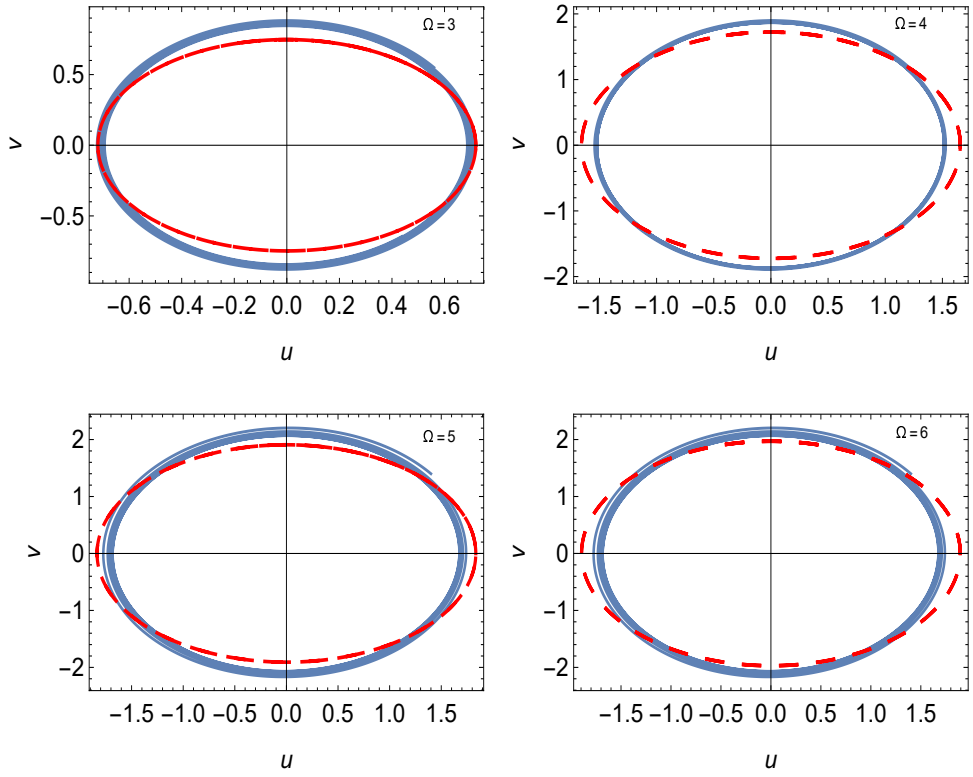

Figure 3.4: Numerical(solid lines) and analytical(dashed line) comparison of limit cycles for different values of $\Omega's$ and for fixed value of fast frequency drive strength g. Simulation is done on Eq. (3.4.1.2 and 3.4.1.3) where the analytical plot based on Eq. (3.4.1.9 and 3.4.1.10).And the related parameters $\gamma = 0.0015, \alpha = 0.0001, c = 0.0005, \omega = \omega_0 = 0.3, h = 0.01$ and $g = 12$.

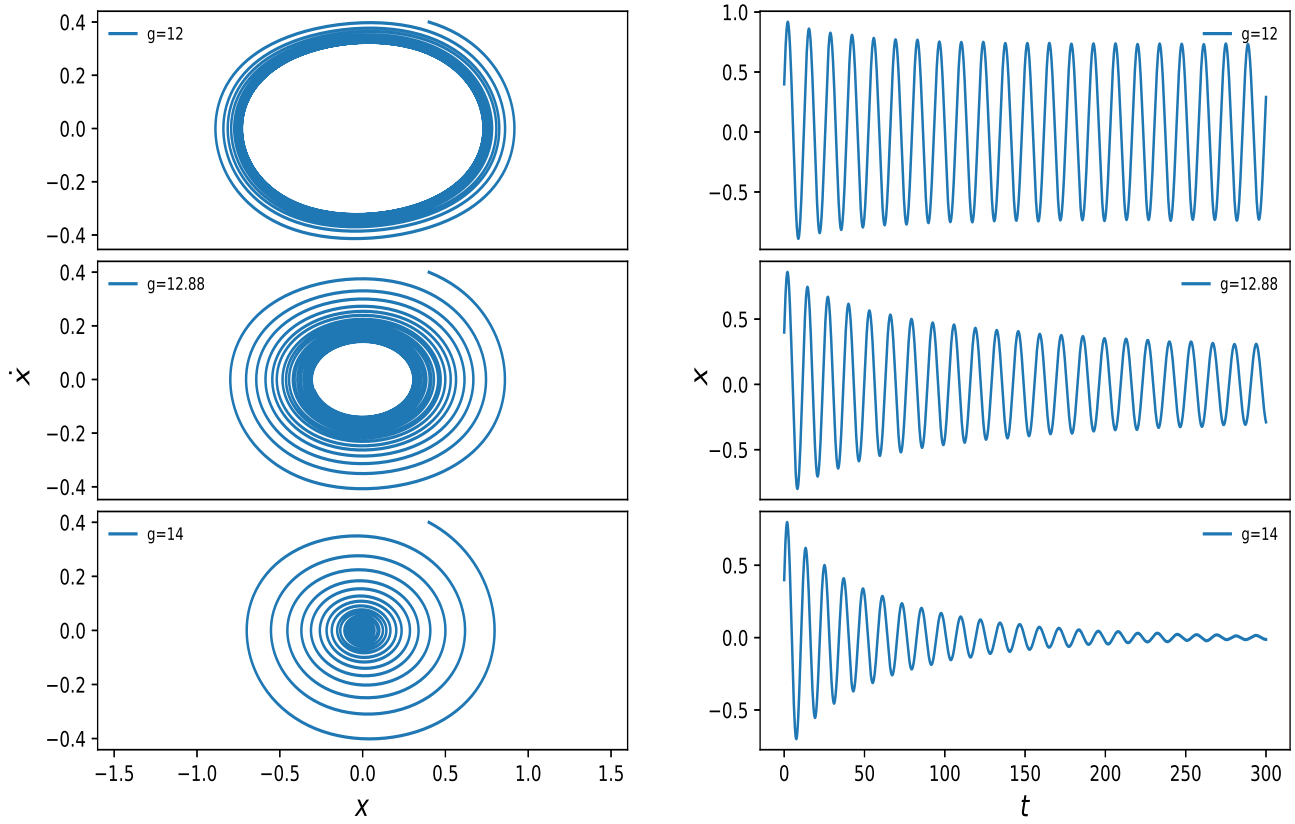

Figure 3.5: Numerical simulation of Supercritical Hopf bifurcation based on Eq. (3.3.1) for $\Omega = 3$. Other parameters are fixed and given by $\gamma = 0.15, \alpha = 0.1, c = 0.0005, \omega = \omega_0 = 0.3$ and $h = 0.01$.Shows a clear transition from stable limit cycle to stable spiral at $g_{hopf} = 12.88$

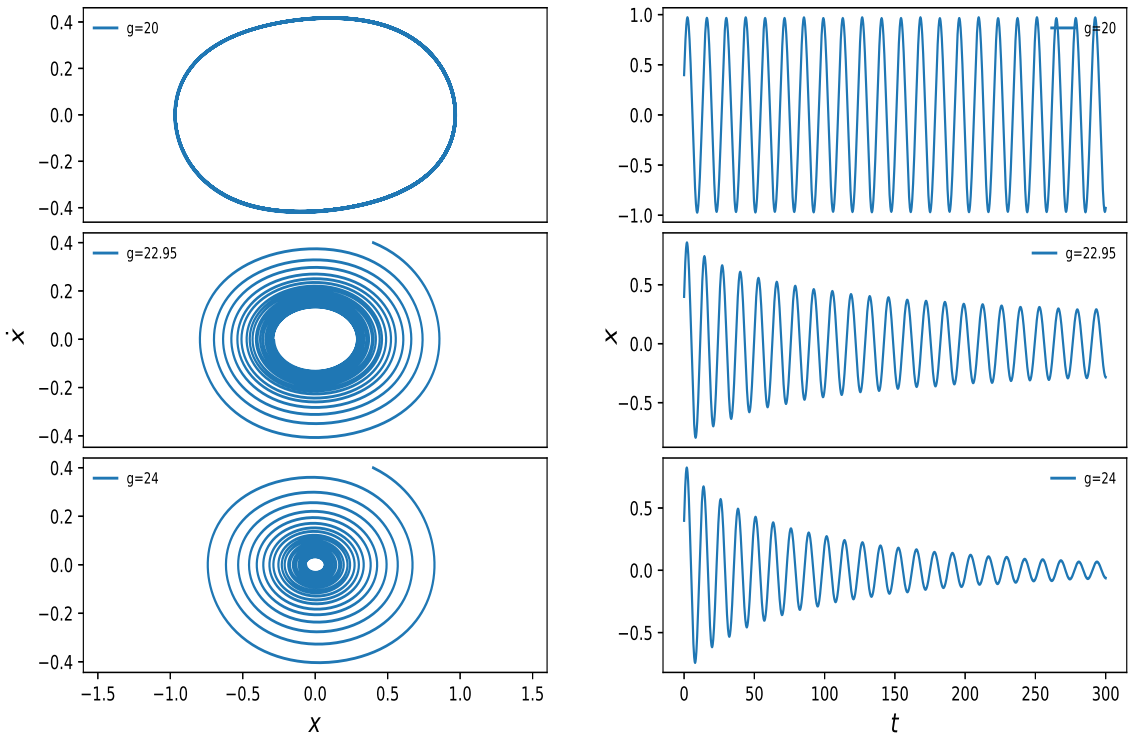

Figure 3.6: Numerical simulation of Supercritical Hopf bifurcation based on Eq. (3.3.1) for $\Omega = 4$. Other parameters are fixed and given by $\gamma = 0.15, \alpha = 0.1, c = 0.0005, \omega = \omega_0 = 0.3$ and $h = 0.01$. Shows a clear transition from stable limit cycle to stable spiral at $g_{hopf} = 22.95$

Chapter 4

Supercritical Hopf Bifurcation in vibrational resonance through modulation of fast frequency

- **Motivation of this Chapter**

  The subject of Vibrational Resonance has burgeoned to a significant volume of literature in nonlinear dynamics over the past two decades. The response of nonlinear systems to two separate driving forces one with slower frequency and the other with a frequency much faster than the former one, has been the standard paradigm for all mod-

els proposed and studied within the ambit of vibrational resonance [10, 11, 12, 13, 14, 15, 16, 17, 18, 19, 20, 21, 22, 23, 24, 25]. In a recent study we have explored the effect of vibrational resonance for a certain parametric oscillator which in the literature has been named Van der Pol-Mathieu-Duffing oscillator. There are two basic motivations behind studying this oscillator. Firstly, as there is already a parametric frequency associated with the oscillator in addition to its own natural frequency, study of vibrational resonance for such an oscillator is usually done by bringing in a single forcing term with very high frequency [44, 45, 46, 47, 34]. Studies pertaining to the response of such systems in presence of an additional forcing term with frequency much slower than the fast drive has therefore been rare. Secondly, due to the spatially nonlinear nature of the damping of a self-excited oscillator, it turns out that the action of these twin forcing terms results in a modification of the damping along with the natural frequency of the oscillator. While the latter phenomenon, where the natural frequency of the system gets modified in the slow dynamics of the oscillator, is a widely addressed issue in the context of vibrational resonance, the former phenomenon, where the damping undergoes a modification, is relatively less explored. It is precisely this phenomenon that gives a supercritical Hopf bifurcation in the oscillator under study. But, the interesting aspect that transpires is, this bifurcation can be effected in two ways: one, by varying the strength of the fast driving term while

keeping the frequency constant, and two, by varying the fast frequency itself while keeping the strength constant. The first procedure is more in keeping with traditional studies of systems showing vibrational resonance and has been studied in detail in a recent communication [52]. The second procedure is the subject of this chapter.

4.1 The model and the flow equations

The model oscillator that we are studying here is given by the following equation:

$$\ddot{x} + \gamma(x^2 - 1)\dot{x} - \omega_0^2(1 + h\cos\omega_p t)x + \alpha x^3 = c\cos\omega t + g\cos\Omega t \qquad (4.1.1)$$

where ω_0 is the natural frequency of the oscillator. The parametric excitation is done through the term $h\cos\omega_p t$ where the magnitude of the parametric frequency will be chosen to be $\omega_p = 2\omega_0$ [52]. On the right hand side of the above equation, there are two driving terms, $c\cos\omega t$ and $g\cos\Omega t$, with the frequency of the latter term much greater than that of the former, viz., $\Omega >> \omega$. When the parameter h, the strength of the parametric drive, falls in the range $-1 < h < 1$ we have a bistable oscillator in unstable equilibrium

on the crest of a double well. The effect of the high frequency drive $g\cos\Omega t$ is to redress this bistability to an effective monostable potential where the system oscillates about a stable equilibrium.

This effective slow dynamics can be derived by first separating the dynamical variable x into a slow variable s and a fast variable f

$$x(t) = s(t, \omega t) + f(t, \Omega t). \tag{4.1.2}$$

The fastness of the variable f gets reflected in the fact that the averages of the odd moments over a complete time period are zero, viz., $\langle f\rangle = \langle f^3\rangle = 0$ while the value of $\langle f^2\rangle$, after some algebra [52] evaluates to $\langle f^2\rangle = Mg^2/2$, where $M = 1/\kappa^2$ with κ given as

$$\kappa = \frac{\Omega^2(\Omega^2+\gamma^2)}{\sqrt{(\Omega^2-\omega_0^2)^2+\Omega^2\gamma^2}} = \frac{1}{\sqrt{M}} \tag{4.1.3}$$

Eventually, all the average effects of the fast variable get incorporated into the equation of the slow variable thus leading to an effective equation for the slow variable as

$$\ddot{s} + \gamma(s^2+K)\dot{s} + (\tilde{\omega}^2 - \omega_0^2 h\cos\omega_p t)s + \alpha s^3 = c\cos\omega t \tag{4.1.4}$$

where the frequency term $\tilde{\omega}$ is given by

$$\begin{aligned}\tilde{\omega}^2(g,\Omega) &= 3\alpha\left\langle f^2\right\rangle - \omega_0^2 \\ &= \frac{3}{2}\alpha g^2 M - \omega_0^2 \end{aligned} \tag{4.1.5}$$

and the factor associated with the nonlinear damping K takes the form

$$K(g,\Omega) = \frac{g^2}{2}M(\Omega) - 1. \tag{4.1.6}$$

Defining an effective frequency as $\omega_{eff} = \sqrt{\tilde{\omega}^2 - \omega_0^2 h\cos\omega_p t}$ we can identify an effective monostable potential $V_{mono}(s,t) = \frac{1}{2}\omega_{eff}^2(t)s^2 + \frac{1}{4}\alpha s^4$. The central fact that merits close observation is that the coefficient of x on the left hand side of Eq.(4.1.1) is negative, while the coefficient of s on the left hand side of Eq.(4.1.4) is positive, provided that, along with the previously imposed condition on h (viz. $-1 < h < +1$), we have an additional condition $-\tilde{\omega}^2 < \omega_0^2 h < \tilde{\omega}^2$.

In Eqs.(4.1.5) and (4.1.6) we have expressed the effective terms $\tilde{\omega}$ and K as functions of the strength g as well as the high frequency Ω of the fast driving force $g\cos\Omega t$. This opens up the scope for studying the consequence of exciting the system with a slow as well as a fast drive in terms of variation not only of g but also of Ω. The effect of the fast drive term is twofold. Firstly, from Eqs.(4.1.4) and (4.1.5) we see that the new frequency $\tilde{\omega}$ emerges as an effective natural frequency replacing ω_0 of Eq.(4.1.1). Secondly, the Van der

Pol damping term gets modified from $\gamma(x^2-1)\dot{x}$ in Eq.(4.1.1) to $\gamma(s^2+K)\dot{s}$ in Eq.(4.1.4). The question of a Hopf bifurcation arises when this effective damping parameter K passes through a zero in course of its variation with respect to either g or M. The effect of the variation in g leading to a Hopf bifurcation has been studied in [52]. Here we are exploring the effect of variation of K as a consequence of variation in M. From the structure of M given in Eq.(4.1.3) it is clear that for large values of Ω we have $M \sim \Omega^{-4}$, a crucial point to which we shall come a little later.

To make further progress we need to derive the amplitude and phase flow equations from Eq.(4.1.4) with the parametric frequency replaced by a value that is twice the value of the slow driving frequency [52], i.e., $\omega_p = 2\omega$. The flow equations can be arrived at through some standard perturbation technique, for example, multiple-time-scale analysis the details of which have been described in [52]. Defining the dimensionless time $\tau = \omega t$, we do the perturbation around the redressed natural frequency $\tilde{\omega}$ by making the frequency ω of the slow forcing drive perturbatively close to $\tilde{\omega}$ through the introduction of a detuning $\tilde{\sigma}$ as $\omega = \tilde{\omega} + \epsilon\tilde{\sigma}$, where ϵ is the perturbation parameter denoting smallness. Introducing the rescaled parameters $\Gamma = \gamma/\omega$, $\Lambda = \alpha/\omega^2$, $C = c/\omega^2$ and $H = h{\omega_0}^2/\omega^2$, we can rearrange Eq.(4.1.4) as

$$s'' + s = \epsilon[-\Gamma(s^2+K)s' + H(\cos 2\tau)s - \Lambda s^3 + C\cos\omega\tau + \sigma s] \qquad (4.1.7)$$

where the rescaled detuning parameter is defined to first order in ϵ as $\tilde{\omega}^2 = \omega^2(1-\epsilon\sigma)$. For using multiple-time-scale analysis we can write the perturbation expansion $s(\tau_0,\tau_1) = s_0(\tau_0,\tau_1) + \epsilon(\tau_0,\tau_1) + \mathcal{O}(\epsilon^2)$ and proceeding as usual [52] we arrive at the amplitude and phase flow equations

$$\frac{da}{d\tau} = -\frac{1}{2}\left[\frac{\Gamma a^3}{4} + \Gamma K a + C\sin\theta + \frac{Ha}{2}\sin(2\theta)\right] \tag{4.1.8}$$

$$\frac{d\theta}{d\tau} = \frac{1}{2}\left[\frac{3\Lambda}{4}a^2 - \sigma - \frac{C}{a}\cos\theta - \frac{H}{2}\cos(2\theta)\right] \tag{4.1.9}$$

The fixed points of these equations obtained by putting the derivatives equal to zero lead us to those specific locations in the parameter space where we can get the nonlinear responses of the system depicted by peaks in the amplitude curve. By parameter space we mean that we can either study the peaks by varying the strength of the fast frequency drive, g, and keeping the other parameter, viz., the high frequency Ω fixed, or we can go the other way round and obtain peaks by varying Ω and keeping g fixed. For more specific details in these lines the interested reader is referred to [52, 59]. We can also use these flow equations to investigate the possibility of creation or destruction of limit cycle through some Hopf bifurcation as one varies either of the parameters g or Ω. For studying the Hopf bifurcation as a result of the variation in the strength g, the reader is again referred to [52]. In the following we shall

study the possibility of Hopf bifurcation as we vary the fast frequency Ω. To the best of our knowledge, this particular investigation has not been done earlier.

4.2 Hopf bifurcation and formation of limit cycle

The question of a limit cycle arises because in the initial equation of motion Eq.(4.1.1) the expression associated with the damping constant γ imparts on the oscillator the capability to self-excite itself. This signature of a Van der Pol damping term leads to a limit cycle through a supercritical Hopf bifurcation. To understand the Hopf bifurcation in the VMD oscillator we are studying here, we have to invoke perturbation theory once again on the flow equations (4.1.8) and (4.1.9) by introducing a new perturbation parameter λ so that the system goes over to a limit cycle over a much longer time-scale given by $t \sim \mathcal{O}(1/\lambda\epsilon)$. This process will lead us to a new set of flow equations which, in the literature, go by the name "super-slow flow" equations [67]. From these flow equations, we can predict with reasonable accuracy, the point in Ω-space where the origin gets destabilized thus giving birth to a stable limit cycle through a supercritical Hopf bifurcation.

The method of multiple-time scale analysis can be best implemented on the flow equations (4.1.8) and (4.1.9) through the pair of substitutions $u = a\cos\theta$

and $v = -a\sin\theta$ leading to the following pair of transformed equations:

$$\begin{aligned}\frac{du}{d\tau} &= (-\frac{\sigma}{2}+\frac{H}{4})v+\lambda\Big\{\frac{1}{8}(3\Lambda v-\Gamma u)(u^2+v^2) \\ &- \frac{\Gamma K u}{2}\Big\} \qquad (4.2.1)\\ \frac{dv}{d\tau} &= (\frac{\sigma}{2}+\frac{H}{4})u+\lambda\Big\{\frac{c}{2}-\frac{1}{8}(3\Lambda u+\Gamma v)(u^2+v^2) \\ &- \frac{\Gamma K v}{2}\Big\} \qquad (4.2.2)\end{aligned}$$

The arrangement of terms in the above two equations has been made such as to guarantee that at the zeroth order both the variables u and v oscillate simple harmonically with the frequency $\omega_l = \sqrt{\frac{\sigma^2}{4}-\frac{H^2}{16}}$. This is a basic requirement because, the perturbation theory that follows is constructed on the basis of these stable oscillations at the zeroth order. Now, with the different time-scales defined as $T_j = \lambda^j\tau$, one can write down the perturbation expansions [47, 55] in the parameter λ as,

$$\begin{aligned}u(T_0,T_1) &= u_0(T_0,T_1)+\lambda u_1(T_0,T_1)+\mathcal{O}(\lambda^2)\\ v(T_0,T_1) &= v_0(T_0,T_1)+\lambda v_1(T_0,T_1)+\mathcal{O}(\lambda^2)\end{aligned} \qquad (4.2.3)$$

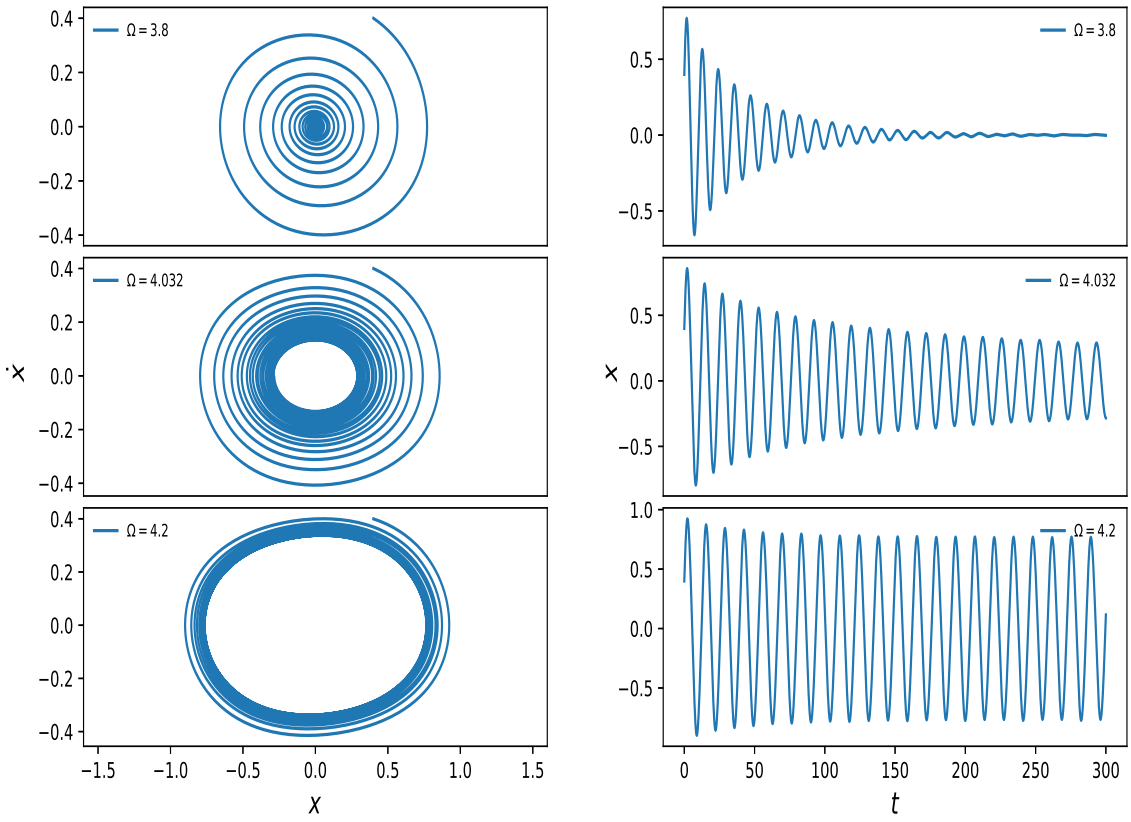

Figure 4.1: Numerical plot of (4.1.7) for *supercritical Hopf* bifurcation: for $g = 23, \Omega_{hopf} = 4.032$. Other parameters are fixed at $\gamma = 0.15, \alpha = 0.1, c = 0.0005, \omega = \omega_0 = 0.3$ and $h = 0.01$.

By iterating these expansions in Eqs.(4.2.1) and (4.2.2) order by order, one can proceed with a standard multiple-time scale analysis [52]. The zeroth order solutions evaluate to

$$u_0 = r(T_1)\cos(\omega_l T_0 + \psi(T_1)) \tag{4.2.4}$$

$$v_0 = \frac{\omega_l}{p} r(T_1)\sin(\omega_l T_0 + \psi(T_1)) \tag{4.2.5}$$

where $p = -(\frac{\sigma}{2} - \frac{H}{4})$. Invoking Eqs.(4.2.4) and (4.2.5) into the first order equations and equating the resonant terms to zero we get the sought after set of ("super-slow") flow equations as

$$D_1 r = \frac{-\Gamma K}{2} r - \frac{\sigma\Gamma}{8\sigma - 4H} r^3 \tag{4.2.6}$$

$$D_1 \psi = -\frac{9\Lambda\sigma^2}{4(2\sigma - H)\sqrt{(4\sigma^2 - H^2)}} r^2. \tag{4.2.7}$$

The two fixed points of the amplitude equation Eq.(4.2.6), one being at the origin $r = 0$, and the other being at

$$r = \sqrt{K\left(\frac{2H}{\sigma} - 4\right)} \tag{4.2.8}$$

gives us the location of a limit cycle, provided the square-root is real. As we have seen above that for stable oscillations at the zeroth order (u_0 and v_0) with frequency $\omega_l = \sqrt{\frac{\sigma^2}{4} - \frac{H^2}{16}}$, we must have $H < 2\sigma$. This implies that in Eq.(4.2.8), *K must be negative for a stable limit cycle to form.* Looking back

at Eq.(4.2.6) we see that $K < 0$ is indeed the requirement for the origin to be unstable in which case it is only this stable limit cycle where the system can go and settle on. When K is positive, on the other hand, we see that there is no limit cycle anywhere, i.e., no real root for r in Eq.(4.2.8), and the system collapses on to a stable origin ($r = 0$). Therefore right at $K = 0$ a stable limit cycle is born through a Hopf bifurcation in the K parameter space. Furthermore, with $H < 2\sigma$, where stable oscillations occur at zeroth order, and on the basis of which this perturbation theory has been built up, we have the coefficient of r^3 on the right hand side of Eq.(4.2.6) as negative thus clearly signaling that the Hopf bifurcation that occurs at $K = 0$ is of the supercritical type.

The specific observation, one that has been alluded to heretofore and we intend to propose through this chapter is that, this continuous variation of K through the Hopf point can be achieved in two ways, either by fixing the fast frequency Ω and varying the strength of the fast drive g, or by fixing g and varying the fast frequency Ω as is clear from the expression for $K \equiv K(g, \Omega)$ appearing in Eq.(4.1.6). For $K = 0$, the Hopf point, we have therefore the relation

$$M_{hopf} = \frac{2}{[g_{hopf}]^2}. \tag{4.2.9}$$

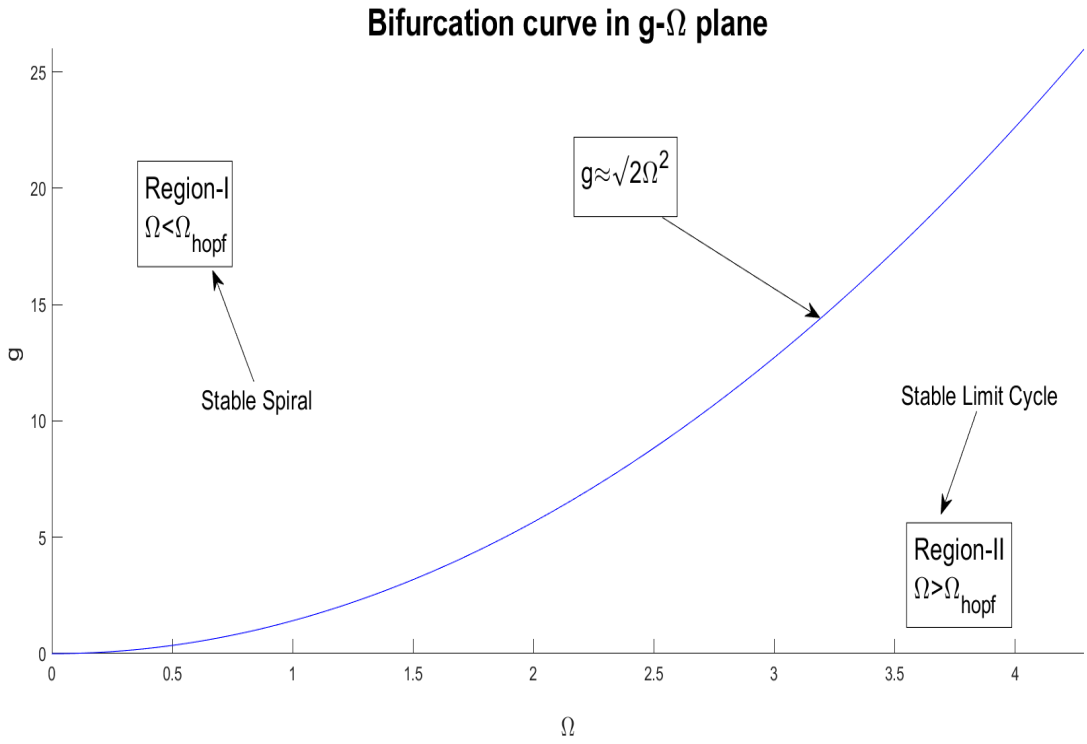

Figure 4.2: Bifurcation curve in $g - \Omega$ plane.Region I indicates the zone of stable nodes and region II implicates the zone of stable limit cycles.

If one plots (not done here) M_{hopf} along the y-axis and g_{hopf} along the x-axis, then one may be misled to think that Eq.(4.2.9) is valid through the entire first quadrant of this $g_{hopf} - M_{hopf}$ plane. That this is not the case should be clear from the fact that this entire calculation is based on the fundamental requirement that Ω is much larger in comparison to γ and ω_0, and hence from Eq.(4.1.3) we get $M \sim \Omega^{-4}$. Accordingly, from Eq.(4.2.9) we get that $g_{hopf} \sim \sqrt{2}\Omega^2_{hopf}$. For large values of Ω therefore, we get the region of validity of Eq.(4.2.9) as the tail part of the flattening $g_{hopf} - M_{hopf}$ curve, where the

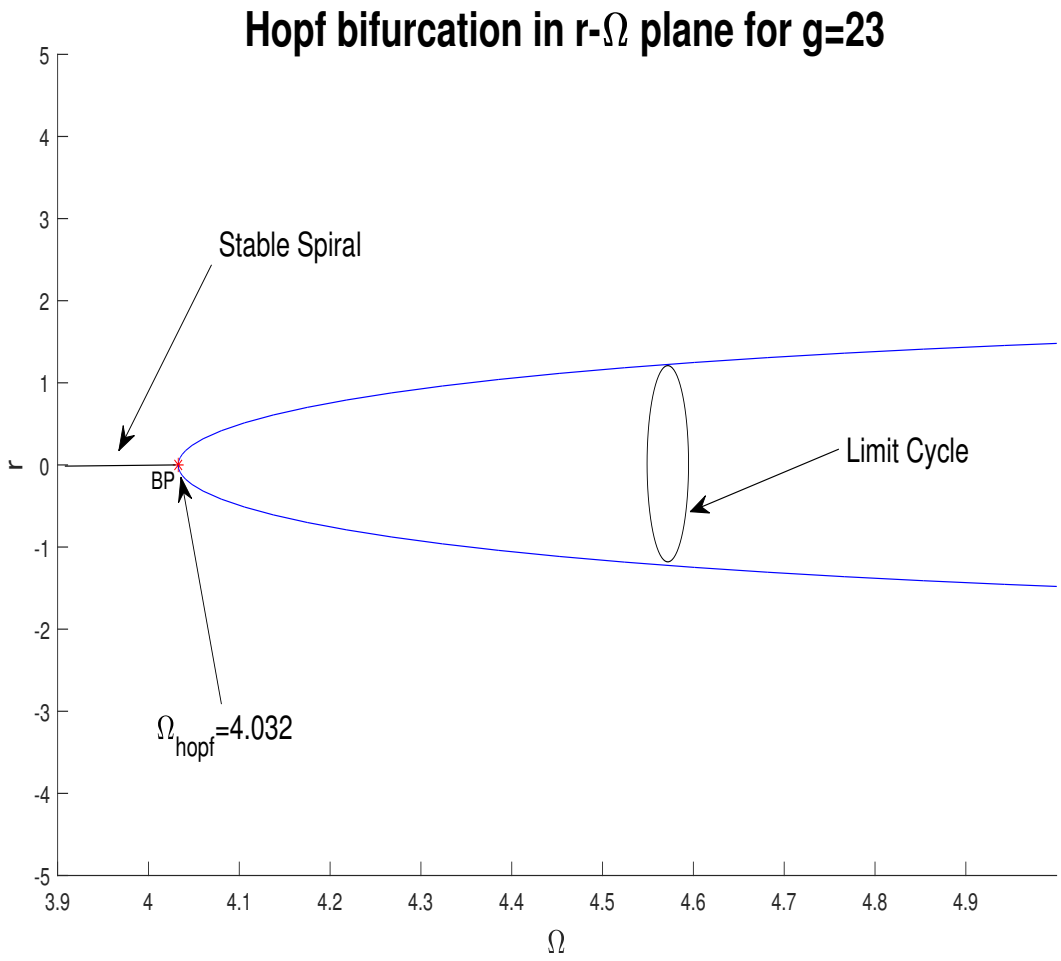

Figure 4.3: Bifurcation curve in $r - \Omega$ plane for $g = 23$ from Eq.(4.2.6). All the other parameters are fixed at $\gamma = 0.0015, \alpha = 0.001, \sigma = 0.1, h = 0.01$. Hopf point is found at $\Omega_{hopf} = 4.032$.

values of g_{hopf} are large while the values of M_{hopf} are small. This confirms our observation that apart from g, the parameter Ω can also play the role of a bifurcation parameter. In studies of bifurcations in context of systems showing vibrational resonance, the role of Ω has been rather confined to being a parameter of much larger value that aids in separating the fast and slow

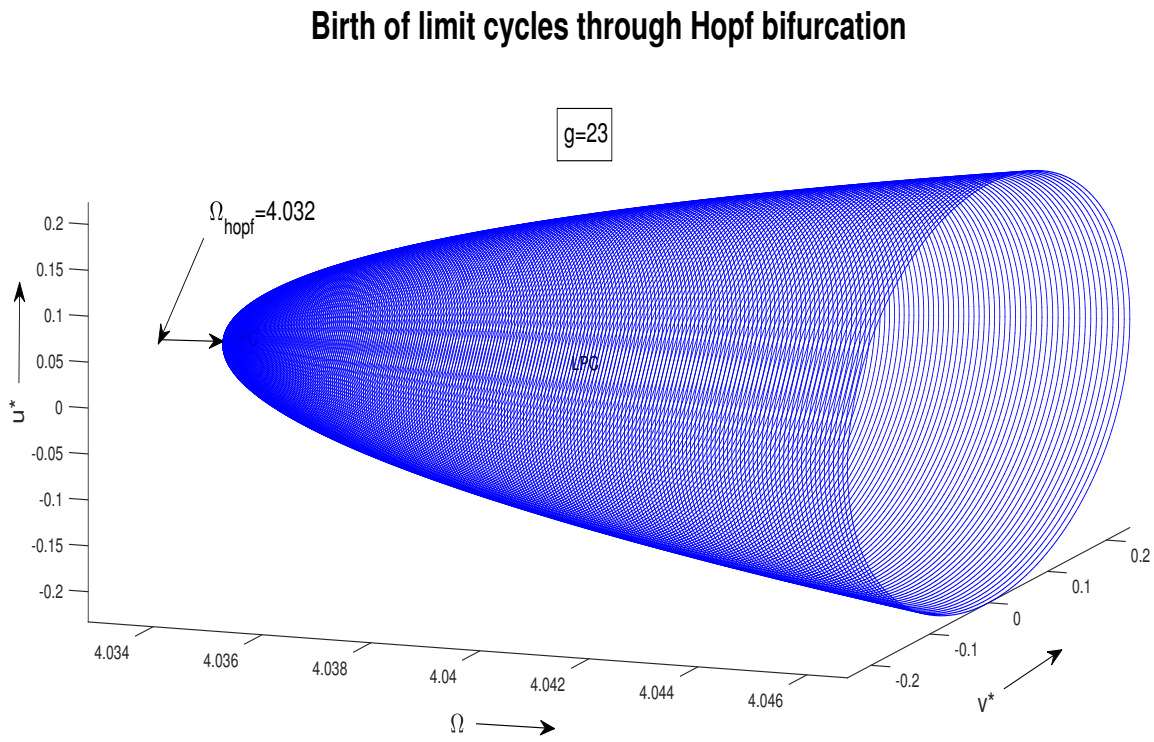

Figure 4.4: Birth of limit cycle at hopf point(3D perspective) is numerically plotted from Eqs.(4.2.1 and 4.2.2).Rest of the parameters are fixed at $\gamma = 0.0015, \alpha = 0.001, \sigma = 0.1, h = 0.01$. Hopf point is found at $\Omega_{hopf} = 4.032$.

dynamics only. But here we see that along the tail part of the $g_{hopf} - M_{hopf}$ curve, owing to the relation $M \sim \Omega^{-4}$, there is a much smaller change in M corresponding to a much larger change in Ω, and hence, one can scan through a significantly long window of Ω values to study a situation where apart from g, the high frequency Ω can cause Hopf bifurcations.

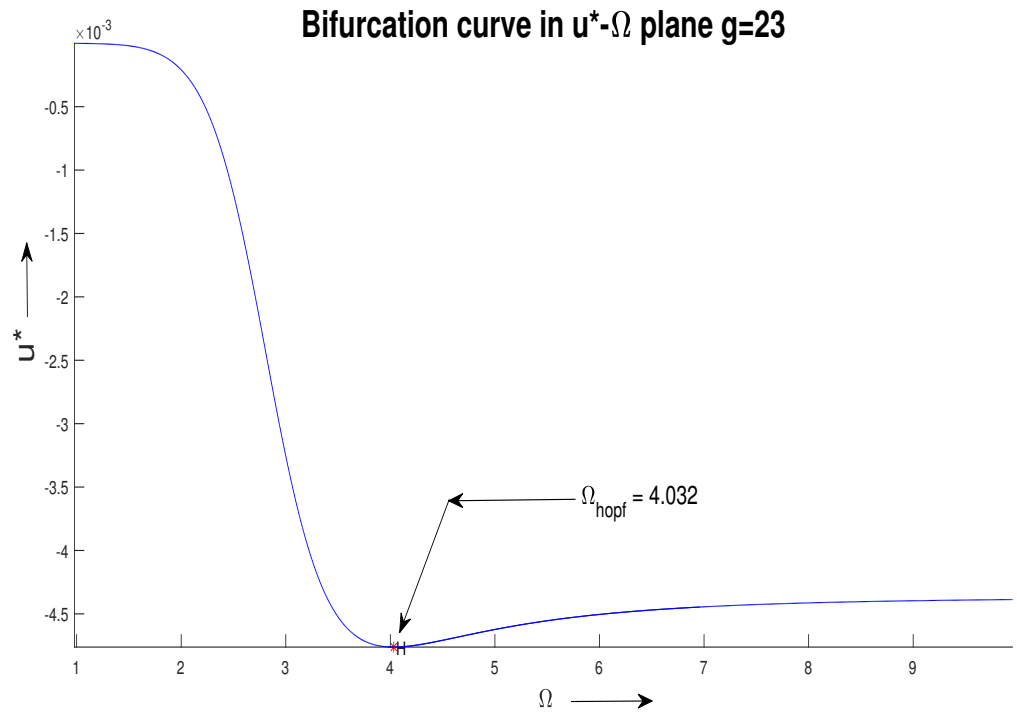

Figure 4.5: Dynamics of fixed point u^* is perceived numerically from Eq.(4.2.1 as we increase Ω .Location of hopf point is denoted by arrow for a fixed g(=23) in $u^* - \Omega$ plane.

4.3 Numerical results

To validate the above analytical results, we have carried out numerical simulations which show quite satisfactory coincide with our study. In (Fig.4.1), it has been displayed that how the change in parameter Ω can destabilize a stable node to give birth of a limit cycle through hopf bifurcation. For a fixed value of $g = 23$ we numerically plot the phase diagram by simulating the original slow flow Eq.(4.1.7), which shows at $\Omega_{hopf} = 4.032$ there is a change

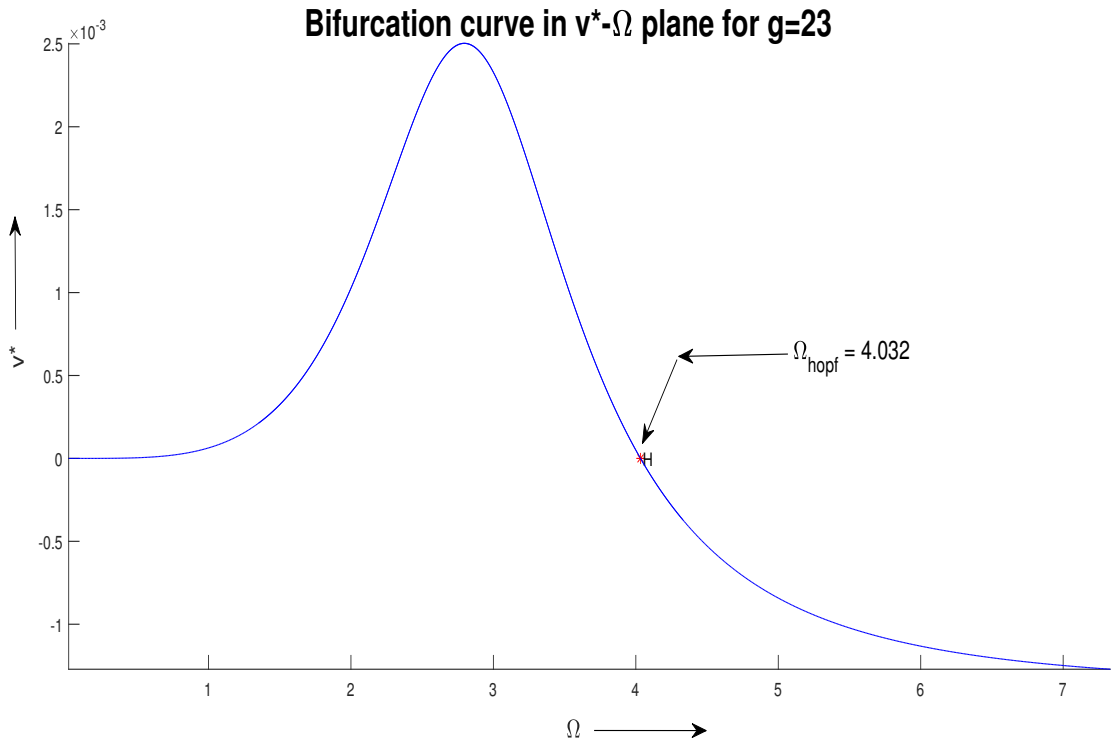

Figure 4.6: Dynamics of fixed point v^* is perceived numerically from Eq.(4.2.2) as we increase Ω .Location of hopf point is denoted by arrow for a fixed g(=23) in $v^* - \Omega$ plane.

in stability through hopf bifurcation. This result is in perfect match with our analytical prediction $g_{hopf} \sim \sqrt{2}\Omega^2_{hopf}$ which is also verified by conducting numerics on Eq.(4.2.1 and 4.2.2), delineated in (Fig.4.2). We have indicated two separate region in this parameter plane $g - \Omega$ region I and II. When a particular value of g is fixed, one can have stable nodes in region I where $\Omega < \Omega_{hopf}$. On the other hand, by crossing the *hopf line*, $g_{hopf} \sim \sqrt{2}\Omega^2_{hopf}$ when we arrive at region II where the condition $\Omega > \Omega_{hopf}$ is satisfied, one can think about the existence of limit cycles. Finally, in (Fig.4.3 and Fig.4.4)

the bifurcation point is pointed out in $r - \Omega$ plane (2D and 3D) by using the Eqs.(4.2.6 and 4.2.7) which is in fact the implementation of "super-slow" flow equations Eqs.(4.2.1 and 4.2.2).We have also portrayed the position of hopf point in the equilibrium plane of (u^*, v^*) separately in (Fig.4.5 and Fig.4.6).

4.4 Summary

To summarize, in this chapter we have explored a new aspect of vibrational resonance in a driven Van der Pol-Mathieu-Duffing oscillator, by showing that apart from treating only the strength of the fast drive as the traditional control parameter to study responses and bifurcations, the fast frequency itself can also be treated as another control parameter. Our main focus here has been to study a supercritical Hopf bifurcation through which the system settles on a stable limit cycle, as result of variation of the fast frequency Ω. We also discuss that owing to very large value of Ω in comparison to other frequencies and the damping constant, only a specific window of the parameter space can be used for studying this phenomenon. We have come to these conclusions by explicitly deriving flow equations for amplitude and phase for both slow and super-slow dynamics through application of multiple-time-scale perturbation theory. The conclusions thus obtained have also been shown to be reasonably consistent with numerical simulations.

Bibliography

[1] L. Gammaitoni, F. Marchesoni, E. Menichella-Saetta, and S. Santucci *Phys. Rev. Lett.* **62**, 349 (1989)

[2] S.Fauve,F.Heslot,*Physics Letters A* , vol **97** (1983)

[3] N G Stocks, N D Stein and P V E McClintock, *J. Phys. A: Math.Gen.* **L385-390** (1993)

[4] J. M. G. Vilar and J. M. Rubí, *Phys. Rev. Lett.* **77**, 2863 (1996)

[5] J. J. Collins, Carson C. Chow, and Thomas T. Imhoff, *Phys. Rev. E.* **52**, R3321(R) (1995)

[6] Arkady S. Pikovsky and Jürgen Kurths, *Phys. Rev. Lett.* **78**, 775 (1997)

[7] R. Löfstedt and S. N. Coppersmith, *Phys. Rev. Lett.* **72**, 1947 (1994)

[8] Milena Grifoni and Peter Hänggi, *Phys. Rev. Lett.* **76**, 1611 (1996)

[9] P. Landa, *Regular and Chaotic Oscillations*,(Springer-Verlag, Berlin, 2001).

[10] P. Landa, P. McClintock, *J. Phys. A* **33**, L433 (2000)

[11] M Gitterman,*J.Phys.A* **34**, L479-L490,(2001)

[12] I.I. Blechman, *Vibrational Mechanics*, (World Scientific, Sin- gapore, 2000)

[13] J. P. Baltanás, L. López, I. I. Blechman, P. S. Landa, A. Zaikin, J. Kurths, M. A. F. Sanjuán, *Phys. Rev. E* **67**, 066119

[14] V. N. Chizhevsky, E. Smeu, G. Giacomelli, *Phys. Rev. Lett.* **91**, 220602 (2003)

[15] B. Knoll,F. Keilmann, *Nature*, volume **399**, pages 134–137 (1999)

[16] S. Jeyakumari, V. Chinnathambi, S. Rajasekar, M. A. F. Sanjuán, *Phys. Rev. E* **80**, 046608 (2009)

[17] S. Rajasekar, K. Abirami, M. A. F. Sanjuán, *Chaos* **21**, 033106 (2011)

[18] C. Jeevarathinam, S. Rajasekar, M. A. F. Sanjuán, *Phys. Rev. E* **83**, 066205 (2011)

[19] S. Jeyakumari, V. Chinnathambi, S. Rajasekar, M. A. F. Sanjuán, *Chaos* **19**, 043128 (2009)

[20] E.Ullner,A.Zaikin,J.García-Ojalvo,R.Báscones,J.Kurths,*Physics Lett.A* **312**,348-354 (2003)

[21] L. Yang, W. Liu, M. Yi, C. Wang, Q. Zhu, X. Zhan, Y. Jia, *Phys. Rev. E* **86**, 016209 (2012)

[22] A. Daza,A. Wagemakers,S. Rajasekar,M.A.F. Sanjuán, *Communications in Nonlinear Science and Numerical Simulation* **18**, 411-416 (2013)

[23] A. Zaikin, L. López, J. P. Baltanás, J. Kurths, M. A. F. Sanjuán, *Phys. Rev. E* **66**, 011106 (2002)

[24] D. Das , D. Ray, *Eur. Phys. J. B* (2018) **91**: 279

[25] S.Ghosh, D.Ray, *Phys. Rev. E.* **88**,042904 (2013)

[26] M.R. Sharma, A.K. Singh, G.S. Benipal, *Latin Am. J. Solids Struct.* **11**, 925 (2014)

[27] N. Yazdi, F. Ayazi, K. Najafi, Proc, *IEEE* **86**, 1640 (1998)

[28] Leone Fronzoni, Michele Giocondo, and Marco Pettini, *Phys. Rev. A* **43**, 6483 (1991)

[29] Juan J. García-Ripoll, Víctor M. Pérez-García, and Pedro Torres, *Phys. Rev. Lett.* **83**, 1715 (1999)

[30] M. D. Lukin, P. R. Hemmer, M. Löffler, and M. O. Scully, *Phys. Rev. Lett.* **81**, 2675 (1998)

[31] Jürgen Berges and Julien Serreau, *Phys. Rev. Lett.* **91**, 111601 (2003)

[32] K.I. Turner, S.A. Miller, P.G. Hartwell, N.C. Macdonald, S.H. Strogatz, S.G. Adams,*Nature* 396, **49** (1998)

[33] J.F. Rhodes, S.W. Shaw, K.L. Turner, J. Moehlis, B.E. DeMartini, W. Zhang, *J. Sound Vib.* **296**, 797 (2006)

[34] Prasun Sarkar, Shibashis Paul and Deb Shankar Ray,*J. Stat.Mech* **2019**,063211 (2019)

[35] Yang J H, Sanjuán M A F, Liu H G and Zhu H, *Nonlinear Dyn.***87**, 172 (2017)

[36] Yang J H, Sanjuán M A F, Liu H G, Litak G and Li X. *Commun. Nonlinear Sci. Numer. Simul.***41**,104 (2016)

[37] Yang J H, Sanjuán M A F and Liu H G, *Eur. Phys. J. B.***88**,310 (2015)

[38] M. Ouni, N. Kahla, A. Preumont, *Eng. Struct.* **45**, 244 (2012)

[39] H. Plat, I. Bucher, *J. Sound Vib.* **333**, 1408 (2014)

[40] V. Kaajakari, A. Lal,*Appl. Phys. Lett.* **85**, 3923 (2009)

[41] M.A. Mironov, P.A. Pyatakov, I.I. Konopatskaya, G.T.Clement, N.I. Vykhodtseva, *Acoust. Phys.* **55**, 567 (2009)

[42] E.R.Rocio, G.R.David, H.R.Richard, *J. Appl. Mech.* 80,050903 (2013)

[43] N.F.Pedersen, M.R.Samuelsen, K.Saermark, *J. Appl.Phys.* **44**, 5120 (2009)

[44] M.Belhaq, A. Fahsi, *Nonlinear Dyn* **53**, 139–152 (2008).

[45] M. Belhaq, S. Sah, *Commun. Nonlin. Sci. Numer. Simul.* **13**, 1706 (2008)

[46] Belhaq, M., Fahsi, A. *Nonlinear Dyn* **57**, 275–287 (2009).

[47] M. Belhaq, M.Houssni, *Nonlinear Dyn.* **18**, 1–24 (1999)

[48] L. Mokni, M. Belhaq, F. Lakrad, *Commun. Nonlin. Sci.Numer. Simul.* **16**, 1720 (2011)

[49] R.H. Huan, W.Q. Zhu, F. Ma, Z.H. Liu, *Shock Vib.* **2014**,792673 (2014)

[50] A. Fidlin, J.J. Thomsen, Int. J. Nonlin. Mech. **43**, 569 (2008)

[51] S.Roy, D. Das, D.Banerjee, *Eur. Phys. J. B* **93**, 12 (2020)

[52] Somnath Roy, Debapriya Das, Dhruba Banerjee,*International Journal of Non-Linear Mechanics*,**135**,103771,ISSN 0020-7462, 2021.

[53] M.Pandey, R.H.Rand, A.Zehnder, *Commun. Nonlinear. Sci. Numer. Simul.* **12**, 1291– 1301 (2007).

[54] M.Pandey, R.H.Rand, A.Zehnder, *Nonlinear Dyn* **54**, 3–12 (2008).

[55] R.H.Rand, K.Guennoun, M.Belhaq, *Nonlinear Dyn.* **31**, 187–193 (2003)

[56] J. Zhang, J. Yang, Z. Zhu, G. Shen, M.A. F. Sanjuán. *International Journal of Bifurcation and Chaos* **30**,06, 2050092 (2020).

[57] J. H.Yang, M. A. F.Sanjuán, H. G. Liu, *Eur. Phys. J. B* **88**, (2015).

[58] J. H.Yang, H. Zhu, *Chaos* **22**, 013112, (2012).

[59] C.Yao, Y.Liu, M.Zhan, *Phys. Rev. E.*, **83**, 061122, (2011)

[60] A. Kimiaeifar. *Mathematical Methods in Applied Sciences.* **33**, 13, 1571-1577, (2010).

[61] RE.Mickens *Oscillations in Planar Dynamics Systems. World Scientific: Singapore*, (1996).

[62] RE.Mickens , AB.Gumel*Journal of Sound Vibration* **250**,955–963, (2002)

[63] Kapitsa P. L, Pendulum with vibrating axis of suspension, Uspekhi fizicheskich nauk, 44, 1 (1954) 7-20 (in Russian).

[64] Kapitsa P. L, Dynamic stability of the pendulum when the point of suspension is oscillating, Jour, of Exper. and Theor. Physics, 21, 5 (1951) 588-597 (in Russian).

[65] D.Jordan, P.Smith, *Nonlinear Ordinary Differential Equations: An Introduction for Scientists and Engineers* (Oxford Texts in Applied and Engineering Mathematics)

[66] A.H.Nayfeh,D.T Mook,*Nonlinear Oscillations*(Wiley-VCH)

[67] S. H. Strogatz,*Nonlinear Dynamics And Chaos: With Applications To Physics, Biology, Chemistry, And Engineering*

Appendix

Derivetion of Eqs.(3.4.1.11) and (3.4.1.12)

Now invoking Eqs.(3.4.1.9) and (3.4.1.10) into Eq. (3.4.1.7) and expanding thr RHS of Eq. (3.4.1.7) term by term also keeping in mind $p = (\frac{\sigma}{2} - \frac{H}{4})$ we get;

1

$$pD_1 v_0 = \omega_l [D_1 r \sin(\omega_l T_0 + \psi) + r \cos(\omega_l T_0 + \psi) D_1 \psi] \tag{A.1}$$

2

$$\frac{p\Gamma K}{2} v_0 = \frac{\omega_l \Gamma K}{2} r \sin(\omega_l T_0 + \psi) \tag{A.2}$$

3

$$\begin{aligned}\frac{p}{8}(\Gamma v_0 u_0^2 + \Gamma v_0^3 + 3\Gamma u_0^3 + 3\Gamma u_0 v_0^2) &= \frac{1}{8}\Bigg[\frac{\Gamma\omega_l r^3}{2}\sin(\omega_l T_0+\psi) - \frac{\Gamma\omega_l r^3}{4}\sin(\omega_l T_0+\psi) \\ &+ \frac{3\Gamma r^3\omega_l^3}{4p^2}\sin(\omega_l T_0+\psi) + \frac{9p\Lambda}{4}r^3\cos(\omega_l T_0+\psi) \\ &+ \frac{3\Lambda\omega_l^2}{2p}r^3\cos(\omega_l T_0+\psi) - \frac{3\Lambda\omega_l^2}{4p}r^3\cos(\omega_l T_0+\psi\Bigg] \\ &= \frac{1}{8}\Bigg[\frac{\Gamma\omega_l r^3}{4}\sin(\omega_l T_0+\psi) + \frac{3\Gamma r^3\omega_l^3}{4p^2}\sin(\omega_l T_0+\psi) \\ &+ \frac{9p\Lambda}{4}r^3\cos(\omega_l T_0+\psi) + \frac{3\Lambda\omega_l^2}{4p}r^3\cos(\omega_l T_0+\psi\Bigg]\end{aligned} \tag{A.3}$$

4

$$-D_0 D_1 u_0 = \omega_l\Bigg[D_1 r\sin(\omega_l T_0+\psi) + r\cos(\omega_l T_0+\psi)D_1\psi\Bigg] \tag{A.4}$$

5

$$-\frac{\Gamma K}{2}D_0 u_0 = \frac{\Gamma K\omega_l}{2}r\sin(\omega_l T_0+\psi) \tag{A.5}$$

6

$$D_0\left[(\frac{3\Lambda v_0}{8} - \frac{\Gamma u_0}{8})(u_0^2 + v_0^2)\right] = \left[(\frac{3\Lambda}{8}D_0 v_0 - \frac{\Gamma}{8}D_0 u_0)(u_0^2 + v_0^2) + (\frac{3\Lambda v_0}{8} - \frac{\Gamma u_0}{8})(2u_0 D_0 u_0 + 2v_0 D_0 v_0)\right] \tag{A.6}$$

From here we now expand the rHS of (A.6) to avoid the clumsy algebraic expression

6a.

$$\frac{3\Lambda}{8}u_0^2 D_0 v_0 = \frac{9\Lambda\omega_l^2}{32p}r^3\cos(\omega_l T_0 + \psi) \tag{A.7}$$

6b.

$$\frac{3\Lambda}{8}v_0^2 D_0 v_0 = \frac{3\Lambda\omega_l^4}{32p^3}r^3\cos(\omega_l T_0 + \psi) \tag{A.8}$$

6c.

$$-\frac{\Gamma}{8}u_0^2 D_0 u_0 = \frac{\Gamma\omega_l}{32}r^3 \sin(\omega_l T_0 + \psi) \tag{A.9}$$

6d.

$$-\frac{\Gamma}{8}v_0^2 D_0 u_0 = \frac{3\Gamma\omega_l^3}{32p^2}r^3 \sin(\omega_l T_0 + \psi) \tag{A.10}$$

6e.

$$\frac{3\Lambda}{4}v_0 u_0 D_0 u_0 = \frac{3\Lambda\omega_l^2}{16p}r^3 \cos(\omega_l T_0 + \psi) \tag{A.11}$$

6f.

$$\frac{3\Lambda}{4}v_0^2 D_0 v_0 = \frac{3\Lambda\omega_l^4}{16p^3}r^3 \cos(\omega_l T_0 + \psi) \tag{A.12}$$

6g.

$$-\frac{\Gamma}{4}u_0^2 D_0 u_0 = \frac{\Gamma\omega_l}{16}r^3\sin(\omega_l T_0 + \psi) \tag{A.13}$$

6h.

$$-\frac{\Gamma}{4}u_0 v_0 D_0 v_0 = -\frac{\Gamma\omega_l^3}{16p^2}r^3\sin(\omega_l T_0 + \psi) \tag{A.14}$$

Here in Eq. (3.4.1.7) we only consider the terms which give the secular terms ,i.e 'sin' and 'cos' terms. These terms will develop unbounded solutions of u_1 and so v_1, which is physically not desirable as the slow dynamics of the oscillator ultimately settled to a steady state oscillation or a damped oscillation. So we equate the coefficients of $\sin(\omega_l T_0 + \psi)$ and $\cos(\omega_l T_0 + \psi)$ equal to zero separately which in turn gives the desired flow equations Eq.(3.4.1.11) and (3.4.1.12).

First equating the coefficients of $\underline{\sin(\omega_l T_0 + \psi)}$ equal to zero gives

$$
\begin{aligned}
2\omega_l D_1 r + \omega_l \Gamma K r + \frac{\Gamma\omega_l}{8} r^3 + \frac{\Gamma\omega_l^3}{8p^2} r^3 &= 0 \\
\implies D_1 r + \frac{\Gamma K}{2} r + \frac{\Gamma r^3}{16}(1 + \frac{\omega_l^2}{p^2}) &= 0 \\
\implies D_1 r + \frac{\Gamma K}{2} r + \frac{\Gamma r^3}{16} \frac{4\sigma}{2\sigma - H} &= 0 \\
\implies \boxed{D_1 r = \frac{-\Gamma K}{2} r - \frac{\sigma\Gamma}{8\sigma - 4H} r^3} &
\end{aligned}
\tag{A.15}
$$

Now equating the coefficients of $\underline{\cos(\omega_l T_0 + \psi)}$ equal to zero gives

$$
\begin{aligned}
2r\omega_l D_1\psi + \frac{9p\Lambda}{32} r^2 + \frac{9\Lambda\omega_l^2}{16p} r^2 + \frac{9\Lambda\omega_l^4}{32p^3} r^2 &= 0 \\
\implies D_1\psi = -\left(\frac{9p\Lambda}{64\omega_l} r^3 + \frac{9\Lambda\omega_l}{32p} r^3 + \frac{9\Lambda\omega_l^3}{64p^3} r^3 \right) & \\
\implies D_1\psi = -\frac{9\Lambda p}{64\omega_l} \left(1 + \frac{\omega_l^2}{p^2} \right)^2 r^2 & \\
\implies D_1\psi = -\frac{9\Lambda p}{64\omega_l} \frac{16\sigma^2}{(2\sigma - H)^2} r^2 & \\
\implies \boxed{D_1\psi = -\frac{9\Lambda\sigma^2}{4(2\sigma - H)\sqrt{(4\sigma^2 - H^2)}} r^2} &
\end{aligned}
\tag{A.16}
$$